N. Jb. Geol. Paläont. Abh. 271/1 (2014), 21–48
Stuttgart, January 2014

Article

Tectonic and palaeogeographic implications of compositional variations within the siliciclastic Ab-Haji Formation (Lower Jurassic, east-central Iran)

Mohammad Ali Salehi, Seyed Reza Moussavi-Harami, Asadollah Mahboubi, Markus Wilmsen and Christoph Heubeck

With 15 figures and 3 tables

Abstract: The Lower Jurassic Ab-Haji Formation which is widespread across east-central Iran but best exposed on the Tabas Block consists of sandstones, siltstones and mudstones deposited in fluvio-deltaic and marginal marine settings. Provenance studies of this formation record the geodynamic history of Central Iran during and in the aftermath of the main Cimmerian event (Triassic–Jurassic boundary to Liassic) and are crucial for the reconstruction of the tectonic setting and palaeogeography of this region. Sandstone provenance analysis of six selected outcrop sections using modal analysis suggests that the predominantly quartzose and quartzolithic sandstones of the Ab-Haji Formation were largely derived from plutonic, quartzose sedimentary and low-grade metamorphic rocks, attributed to a recycled-orogen and cratonic sources. Sandstone and shale geochemistry suggests that most major and trace element patterns are near upper continental crust values, indicating felsic and (meta-) sedimentary sources. Key elemental ratios are consistent with a mixed recycled source under humid climatic conditions and moderate to intensive chemical weathering. Weathering indices indicate that recycling processes and/or humid climatic conditions contributed to the high compositional maturity of the sandstones such that they plot in craton-interior and passive-margin fields on tectonic QtFL and QmFLt ternary diagrams. Paleogeographic reconstructions and geologic mapping indicate that the erosion of uplifted pre-Jurassic rocks exposed in tilted fault blocks within an extensional continental retro-arc basin provided the principal sources. Strata of the Ab-Haji Formation in the western and southern Tabas Block were predominantly derived from low-grade metamorphic and sedimentary rocks exposed on the adjacent Yazd Block, while those in the eastern Tabas and western Lut blocks were derived from the erosion of mature sedimentary strata of the uplifted Shotori Swell, i.e., from the eastern margin of the tilted Tabas Block.

Key words: Sandstone petrography; geochemistry; provenance; extensional basin; Ab-Haji Formation; east-central Iran.

1. Introduction

The principal objective of provenance analysis is to reconstruct source area geology, source-to-sink transport processes, tectonics and climate (Ibbeken & Schleyer 1991). Several standard methods have been developed for the analysis of sandstones (Dickinson & Suczek 1979) and whole-rock geochemistry of fine-grained siliciclastic rocks (Bhatia 1983; Bhatia & Crook 1986). The motivation for sedimentary provenance studies is commonly the intent to understand the dominant controls of sediment-forming processes (e.g. tectonic, climatic, or transport) in the hinterland, to improve the tectonic model of sedimentary basin formation and to predict porosity and permeability trends as a function of source composition. Combined geochemical and petrographic analyses are a powerful tool to reach these objectives. Here, we apply these

DOI: 10.1127/0077-7749/2014/0373
www.schweizerbart.de
0077-7749/2014/0373 $ 7.00

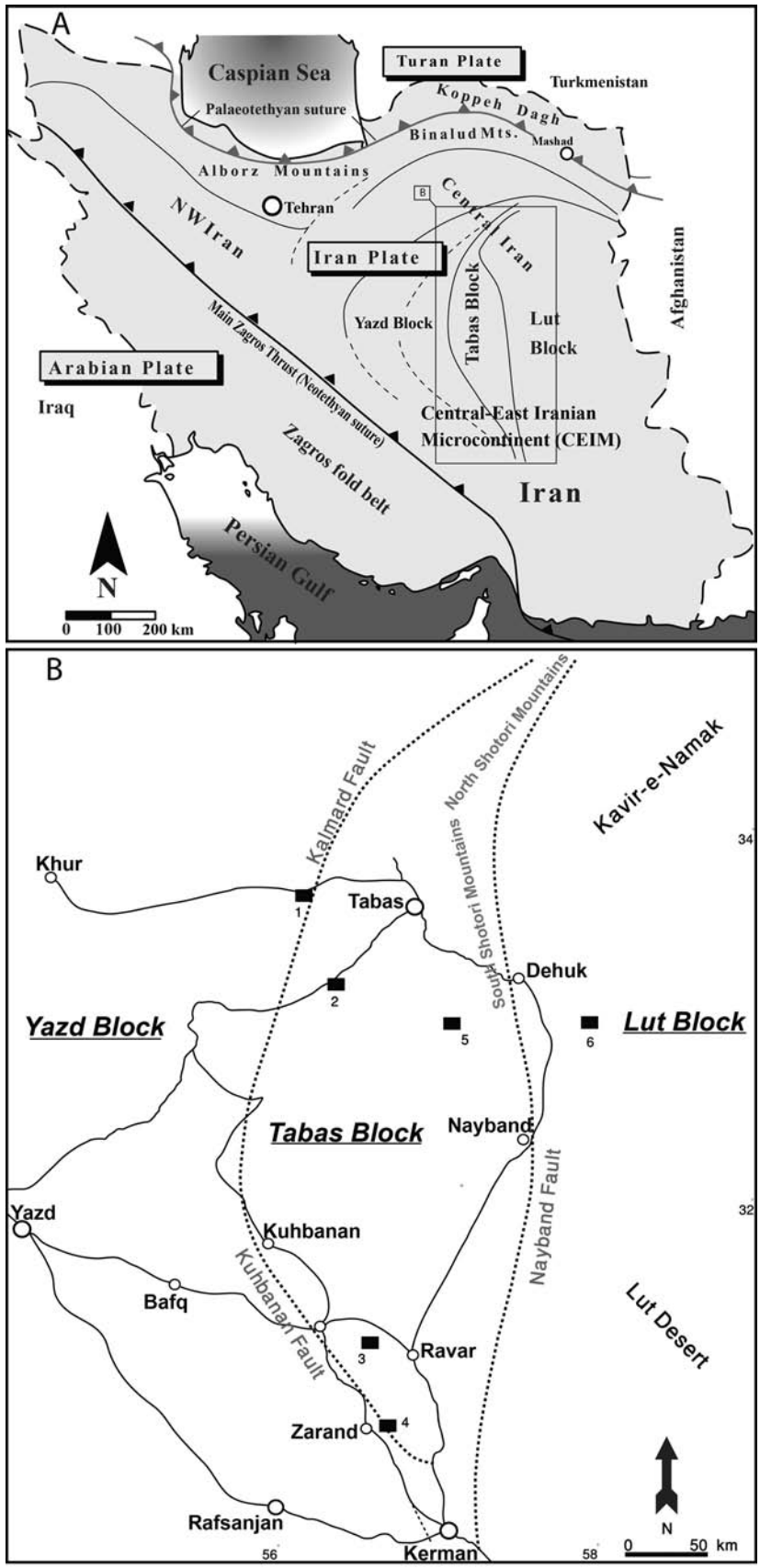
A
Caspian Sea
Turan Plate
Turkmenistan
Palaeotethyan suture
Koppeh Dagh
Binalud Mts.
Mashad
Alborz Mountains
Tehran
B
Central Iran
NW Iran
Iran Plate
Afghanistan
Yazd Block
Tabas Block
Lut Block
Main Zagros Thrust (Neotethyan suture)
Arabian Plate
Iraq
Central-East Iranian Microcontinent (CEIM)
Zagros fold belt
Iran
Persian Gulf
N
0 100 200 km
B
Kalmard Fault
North Shotori Mountains
South Shotori Mountains
Kavir-e-Namak
Khur
Tabas
Dehuk
Yazd Block
Lut Block
Tabas Block
Nayband
Yazd
Kuhbanan
Kuhbanan Fault
Nayband Fault
Bafq
Ravar
Lut Desert
Zarand
Rafsanjan
Kerman
N
0 50 km
34
32
56
58

Fig. 1.

techniques to explore the provenance and tectonic setting of the Lower Jurassic Ab-Haji Formation, east-central Iran. In this region, a number of petrographic and geochemical studies have led to an improved understanding of the tectonic setting and climatic situation in the sedimentary basins of Iran (e.g., Balini et al. 2009; Najafzadeh et al. 2010; Etemad-Saeed et al. 2011).

The development of the Mesozoic sedimentary basins on the Central-east Iranian Microcontinent (CEIM) can be related to the onset of Neotethys subduction at the southern margin of the Iran Plate (Arvin et al. 2007; Wilmsen et al. 2009a; Mahmoudi et al. 2010). This event resulted in continental back-arc extension on the Iran Plate leading to the formation of extensional basins such as the Late Triassic Nayband Basin (Fürsich et al. 2005a), associated with widespread transgressions. Extension resulted in the development of several large Mesozoic back-arc basins along the Eurasian margin (Stampfli & Borel 2002; Brunet et al. 2003; Golonka 2004; Mahmoudi et al. 2010). At the same time, the main Cimmerian uplift and foreland deformation event occurred in northern Iran (Alborz Range) (Wilmsen et al. 2009a) (Fig. 1A).

During the Early Jurassic, the sediments comprising the Ab-Haji Formation were deposited within a segmented continental back-arc basin in east-central Iran (Wilmsen et al. 2009a; Salehi 2013; Salehi et al. subm.). Although the provenance and tectonic setting of this formation have not been evaluated in a regional context, modal analyses of sandstones from the Ab-Haji Formation, limited to the southern part of the Tabas Block (Shadan & Hosseini-Barzi 2013), suggest a recycled-orogen source of a fold-and-thrust belt and deposition into a nearby foreland basin lacking a volcanic contribution, rather than into a back-arc setting. Moreover, major-element discrimination diagrams suggest a quartzose sedimentary provenance reflecting the recycled source. However, an active continental margin setting is suggested for this formation based on limited sandstone and shale geochemistry (Moosavirad et al. 2011, 2012).

Earlier studies (Alikhasi 2008; Shadan & Hosseini-Barzi 2013) focusing on the western and southern parts of the Tabas Block document recycled sources mixed with a minor felsic source. However, volcanic sources for the sediments, which would support a back-arc setting, as well as the sandstone petrography and shale geochemistry of the Ab-Haji Formation in the eastern part of the Tabas and the western Lut blocks, have not been identified (Fig. 1B). The aim of the present study is to evaluate the tectonic setting of the Early Jurassic sediments in east-central Iran through modal analyses of sandstones and the geochemistry of sandstones and shales from the Lut, Tabas and Yazd blocks (Fig. 1B).

2. Geological setting

The Iran Plate, an element of the Cimmerian microplate assemblage, became detached from Gondwana during the Permian and collided with the Turan Plate of Eurasia during the Late Triassic, thereby closing the Palaeotethys (Eo-Cimmerian event; e.g., Stöcklin 1974; Stampfli & Borel 2002; Fürsich et al. 2009a; Wilmsen et al. 2009a) (Fig. 2A). This Eo-Cimmerian Orogeny transformed the northern margin of the Iran Plate into an under-filled Carnian–Rhaetian flexural foreland basin (Wilmsen et al. 2009a). At the same time, Neotethys subduction commenced along the southern margin of the Iran Plate. This process is inferred to have reduced the compression of the Iran Plate such that extensional basins formed. These were subsequently filled with up to 3000 m of marine Norian–Rhaetian-age sediments (Nayband Formation of Central Iran; Fürsich et al. 2005a). The main Cimmerian uplift and foreland deformation event occurred at the Triassic–Jurassic boundary, followed by rapid denudation of the Cimmerian Mountains in northern Iran. This event also resulted in the end of marine sedimentation, followed by a period of non-deposition/erosion, source-area rejuvenation and the deposition of the Lower Jurassic Ab-Haji Formation in east-central Iran (Wilmsen et al. 2009b) (Fig. 2B-C).

Fig. 1. A. Structural and geographic framework of Iran showing main sutures, structural units and geographic areas. B. Locality map of east-central Iran with major structural units (blocks and block-bounding faults; modified from Wilmsen et al. 2009b). Outcrop locations are indicated by black rectangles. 1. Kuh-e-Rahdar. 2. Simin-Sepahan. 3. Ravar-Abkuh. 4. Zarand-Chenaruyeh. 5. Parvadeh. 6. Kuh-e-Shisui.

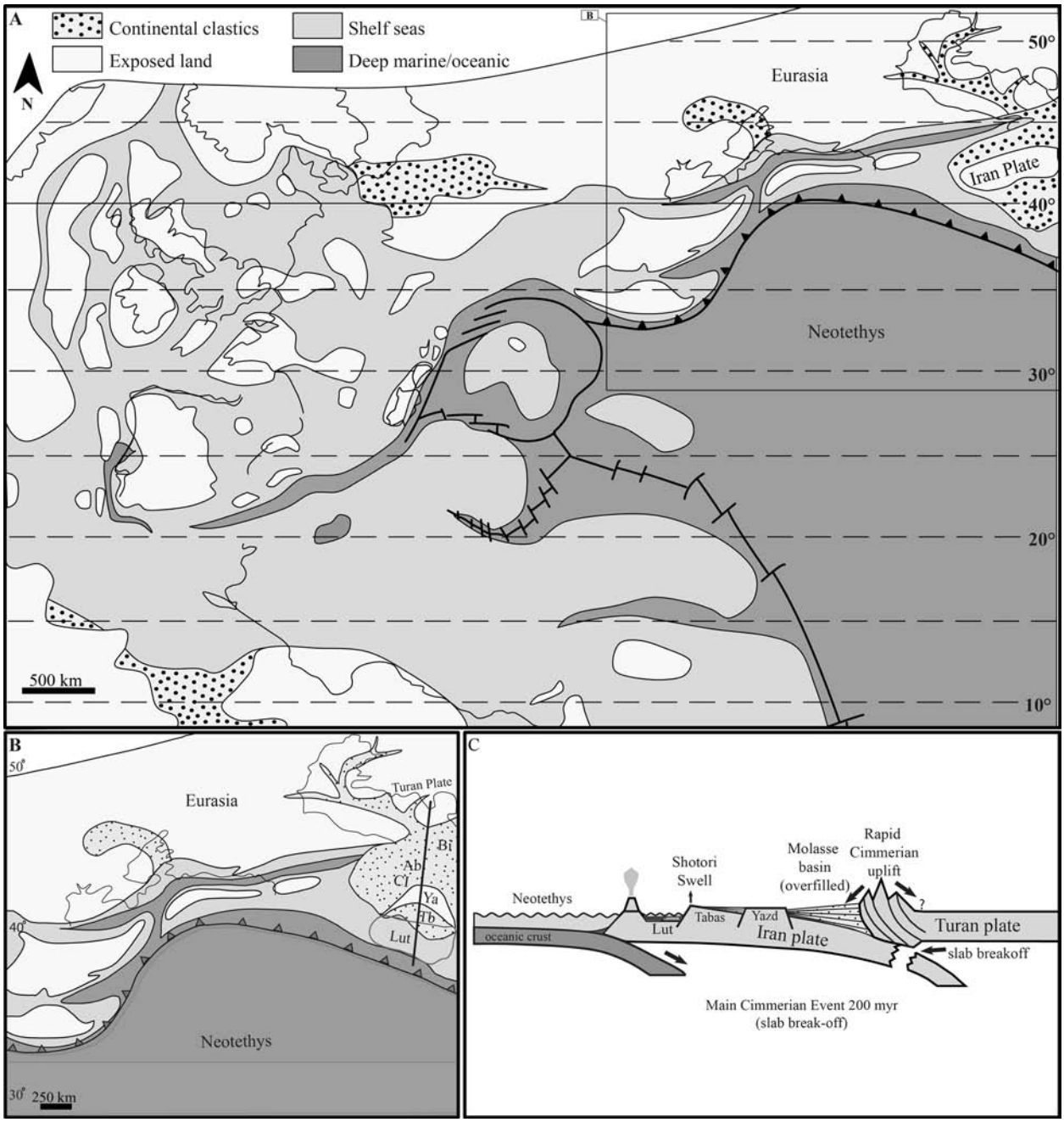

Fig. 2. A. Early Jurassic palaeogeography of the central and western Tethys (modified after THIERRY 2000). B. Lut, Tabas and Yazd blocks are shown in assumed Early Jurassic orientation based on an Early Jurassic palaeogeography of the western Tethys (base map modified after THIERRY 2000). Ab Alborz, CI Central Iran, Tb Tabas, Ya Yazd, Bi Binalud. C. Geodynamic model after the main-Cimmerian event in Iran during the earliest Jurassic (modified from WILMSEN et al. 2009a).

Palaeogeographic reconstructions of the Early Jurassic (THIERRY 2000) place the Iran Plate at the northern margin of the Neotethys at a palaeolatitude of ca. 40°-45°N in a warm-temperate climate (Fig. 2A). The distribution of marine and non-marine strata indicates that the Lut and some part of the Tabas blocks were mostly covered by the sea during the Early Jurassic whereas most of the Yazd Block remained

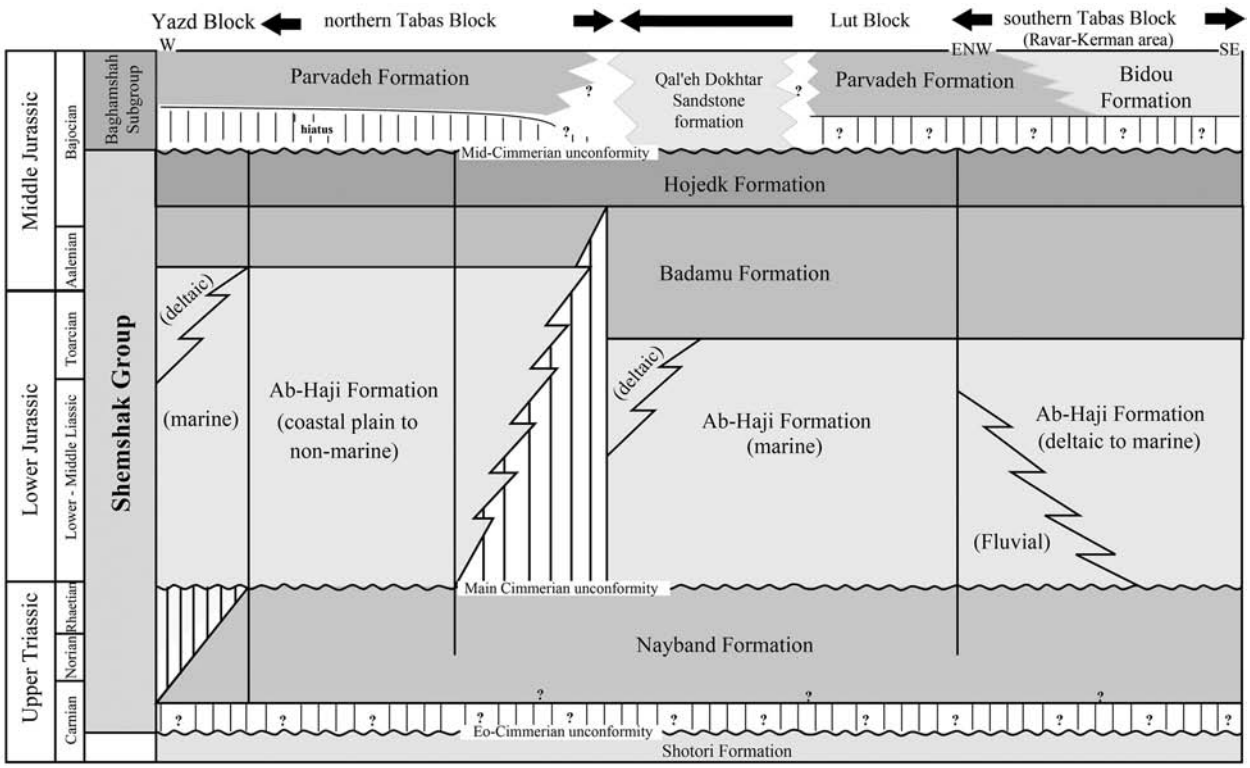

Fig. 3. Lithostratigraphic framework of the Lower-Lower Middle Jurassic System of the northern and southern Tabas Block and the western Lut Block, east-central Iran (modified from Wilmsen et al. 2009a).

emergent (Lower Jurassic stratigraphic gap) (Fig. 2A-B). The common presence of fossil plant fragments and the occurrence of locally mineable coal seams in the Lower Jurassic strata of east-central Iran (Wilmsen et al. 2009b; Alizadeh et al. 2011) confirm a humid-temperate climate with ample vegetation.

Evidence of the Mid-Cimmerian Bajocian-age tectonic event is observed across of the Iran Plate (northern and east-central Iran), where it is documented by conspicuous inter-regional, in part angular, unconformities. Their origin can be related to plate-tectonic processes in the South Caspian area (Brunet et al. 2003; Fürsich et al. 2009b) and along the southern margin of the Iran Plate (Wilmsen et al. 2009b). On the Tabas Block, the Mid-Cimmerian unconformity is well developed and associated with considerable erosion and, locally, gentle folding (Wilmsen et al. 2003; Wilmsen et al. 2009b). The Late Cimmerian event (Late Jurassic–earliest Cretaceous) resulted in intensive block-faulting in east-central Iran (Wilmsen et al. 2010; Cifelli et al. 2013).

Published geodynamic models (e.g., Davoudzadeh et al. 1981; Soffel & Forster 1984; Soffel et al. 1996; Alavi et al. 1997; Besse et al. 1998) have suggested that the CEIM experienced post-Triassic counterclockwise rotation (135°) around a vertical axis to its present-day position, and that this rotation was associated with considerable lateral movements along the block-bounding faults (Figs. 1A and 2B). Rotation took mainly place in post-Jurassic times (Esmaeily et al. 2007; Bagheri & Stampfli 2008; Wilmsen et al. 2009b) although the timing has been questioned by some recent studies (e.g., Muttoni et al. 2009) . Nevertheless, Cifelli et al. (2013) recently suggested that the block-bounding fault between the Tabas and Lut blocks changed from a extensional regime during the Jurassic to a right-lateral transpressional regime between the Early Cretaceous and the Palaeocene. Furthermore, Mattei et al. (2012) have documented evidence of significant Neogene anticlockwise rotation (20°-35°) of the Tabas and Yazd blocks.

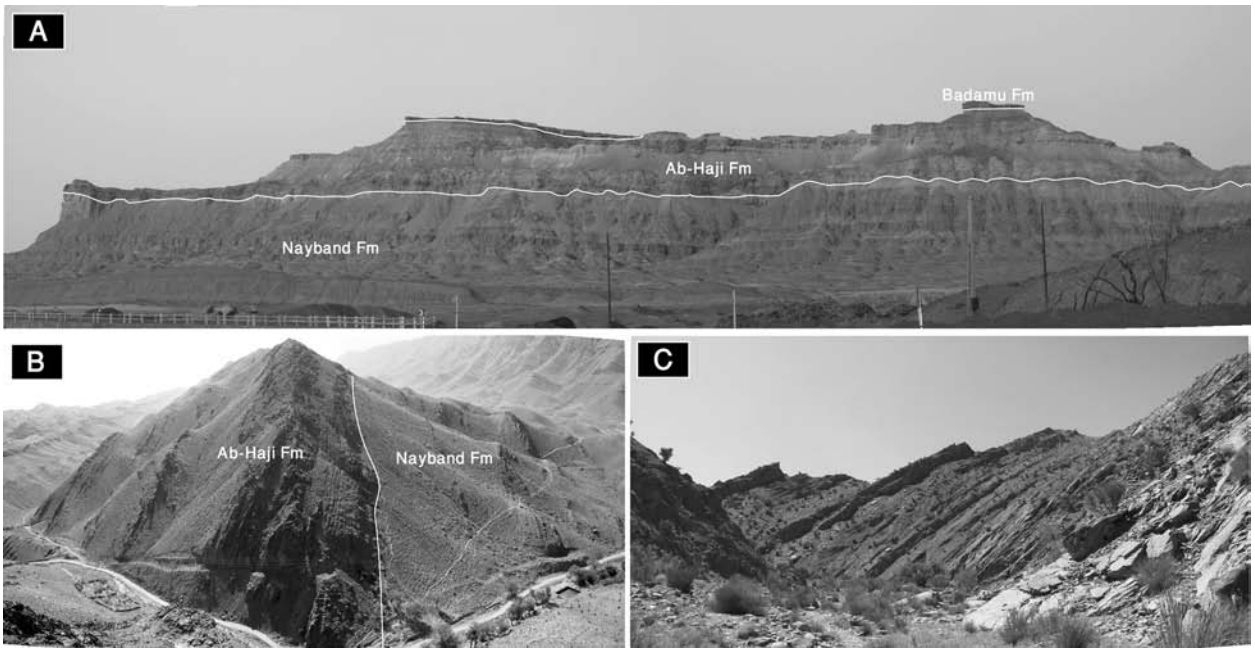

Fig. 4. Field aspects of the Ab-Haji Formation. A. Overview of the Parvadeh section (5), view to the south from the top of the Upper Triassic Nayband towards the Lower Jurassic Ab-Haji and Badamu formations. B. Sharp erosional contact of coarse-grained sandstones of the Ab-Haji Formation overlying fine-grained siltstones and sandstones of the Nayband Formation (Zarand-Chenaruyeh; section 4). Up-section (image left) fine-grained siliciclastics of the Ab-Haji Formation follow. View to the east. C. Close-up photograph of the middle part of the Ab-Haji Formation (Ravar-Abkuh; section 3); the red and gray siltstones and shales between sandstones likely formed in a continental setting.

3. Regional Upper Triassic–Middle Jurassic stratigraphy

As elsewhere on the Iran Plate, Middle Triassic platform carbonates in east-central Iran (Shotori Formation) pass upwards into the overlying Norian-Bajocian siliciclastic rocks of the Shemshak Group (Seyed-Emami 2003; Fürsich et al. 2005a; Fürsich et al. 2009a). This group is delineated by the Eo-Cimmerian unconformity at its base and the Mid-Cimmerian unconformity at its top (Fig. 3).

In all of the studied areas (easternmost Yazd Block, northern and southern Tabas Block, Lut Block), the Upper Triassic Nayband Formation of the lower Shemshak Group is well developed (Figs. 3 and 4A). This widespread formation consists mainly of fine-grained marine siliciclastics and carbonates containing abundant fossils (Hautmann 2001; Fürsich et al. 2005a, Senowbari-Daryan et al. 2010; Hautmann et al. 2011). Upsection the Nayband Formation is overlain by siliciclastic strata of the Lower Jurassic Ab-Haji Formation. The type area of this formation is located in the Kalmard area near Kuh-e-Rahdar, northwestern Tabas Block (Aghanabati 1975), where, however, it is only 82 m thick (Fig. 1B).

The Ab-Haji Formation crops out from the eastern margin of the Yazd Block and within much of the Tabas Block, except along its eastern margin (Shotori Mountains), and extends as far as the western Lut Block (Fig. 3). It attains a thickness of up to 700 m but locally may be reduced to a few tens of meters. Over much of the Tabas Block, the basal contact is marked by coarse-grained quartzarenites (Fig. 4A, B). The Ab-Haji Formation mainly consists of thin- to thick-bedded greenish sand- and siltstones and locally contains rare thin coal seams (Figs. 4C, 5), representing fluvial plain, coastal plain, delta and shallow-marine deposition (Fig. 3) (Salehi 2013; Salehi et al. subm.).

During the Aalenian (in the southern Tabas Block and on the Lut Block already in the Toarcian; Seyed-Emami 1971; Seyed-Emami et al. 2000; Seyed-Emami et al. 2004a), a pronounced transgression initiated the

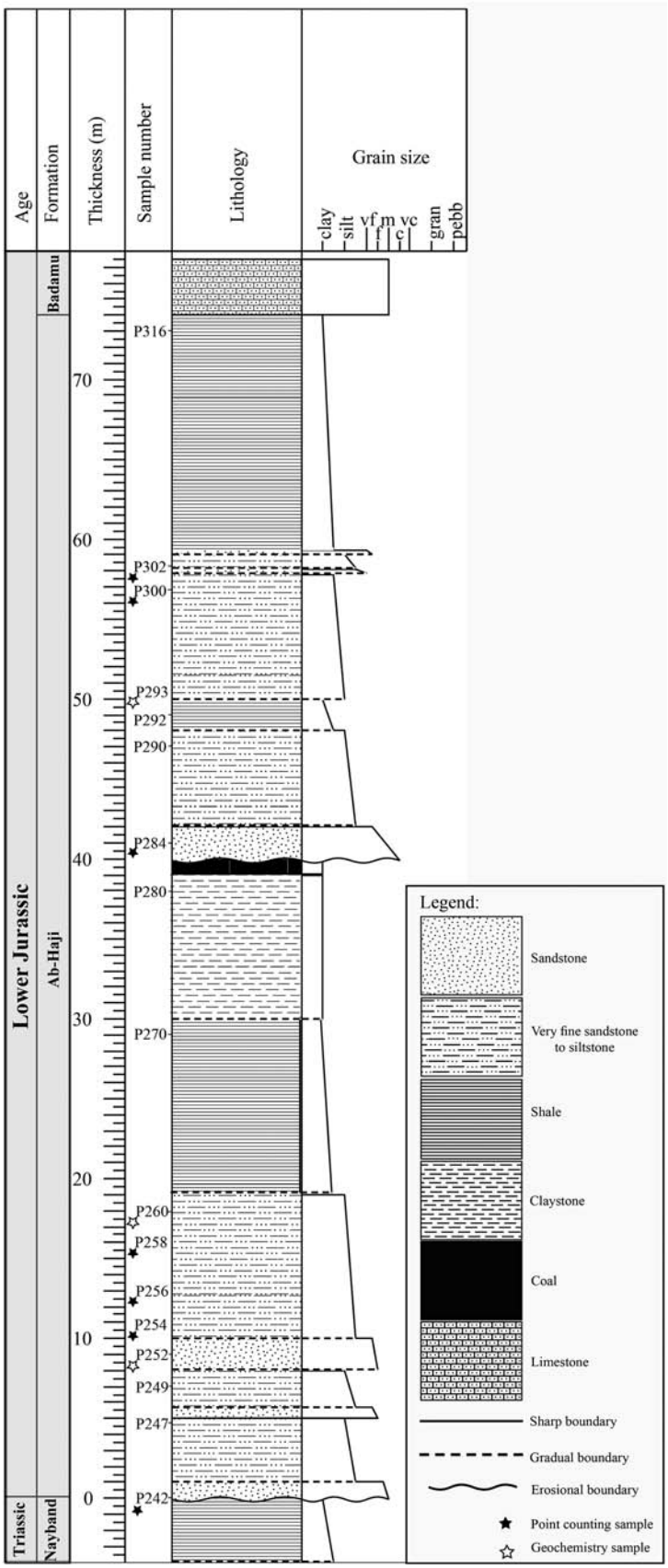

Fig. 5. Representative lithostratigraphic log of the Ab-Haji Formation with sample locations (Parvadeh; section 5). Grain-size code: vf: very fine-; f: fine-; m: medium-; c: coarse-; vc: very coarse-grained sand.

Table 1. Framework parameters of detrital modes (Ingersoll & Suczek 1979).

Qm non	Non-undulose monocrystaline quartz
Qm un	Undulose monocrystalline quartz
Qpq 2-3	Qpq 2-3 crystal units per grain
Qpq > 3	Qpq > 3 crystal units per grain
Cht	Chert
Qp	polycrystalline quartzose (or chalcedonic) lithic fragments (Qpq + Cht)
Qt	Total quartzose grains (Qm + Qp)
Q	Total (Qm non + Qm un) and Qpq used for Folk (1974) classification (Qm +Qpq)
P	Plagioclase feldspar
K	Potassium feldspar
F	Total feldspar grains (P + K)
Lv	Volcanic-metavolcanic rock fragments
Ls	Sedimentary rock fragments
Lm	Metasedimentary rock fragments
L	Unstable (siliciclastic) lithic fragments (Lv + Ls + Lsm)
Lt	Total siliciclastic lithic fragments (L + Qp)
RF	Total unstable rock fragments and chert used for Folk (1974) classification

deposition of the comparatively condensed, ammonite-rich, dark, often oolitic limestones, marls and siliciclastic rocks of the Badamu Formation (Fig. 3).

The overlying Lower Bajocian Hojedk Formation is usually easily identified as the siliciclastic package between the carbonates of the underlying Badamu and the overlying Parvadeh Formations. Its top represents the Mid-Cimmerian unconformity. In the eastern part of the Tabas Block and on the Lut Block, the Hojedk Formation is generally marine and can be dated using ammonites (e.g., Seyed-Emami et al. 2004a). Towards the west, its character changes to marginal marine and fluvial and includes coal seams. The Hojedk Formation is also characterized by rapid lateral facies and thickness changes.

The pronounced transgression following the middle Bajocian Mid-Cimmerian unconformity initiated deposition of the Upper Bajocian to Lower–Middle Bathonian, condensed oncolitic–microbial limestones and siliciclastic rocks of the Parvadeh Formation (30 to 150 m thick; Wilmsen et al. 2009a) which were deposited across wide areas of the Tabas Block and also onlap the Shotori High (Fig. 3). In the western part of the Lut Block, the Parvadeh Formation is replaced by the marine sandstones of the informal Qal'eh Dokhtar Sandstone; in the southern Tabas Block, by the lower part of the lithologically variable Bidou Formation.

4. Methods

More than 600 samples were collected from six outcrop sections of the Ab-Haji Formation in east-central Iran (see Fig. 1B for the locations and outcrop names, Fig. 5 for a representative lithostratigraphic log with sample locations). The texture, fabric and composition of 200 thin sections were studied using optical microscopy. A total of 42 fresh sandstone samples were point-counted following the Gazzi-Dickinson method (Gazzi 1966, Dickinson 1970, Ingersoll et al. 1984). In each thin section, 300 framework grains were counted. Following the convention of Pettijohn (1975), we assigned grains <0.03 mm to the matrix category. Tables 1 and 2 show framework parameters (Ingersoll & Suczek 1979) and detrital mode of sandstones from the Ab-Haji Formation.

Table 2. Detrital modes of 42 selected sandstone samples from the Ab-Haji Formation in east-central Iran.

	Sample	Outcrop No.	Qm non	Qm un	Qp 2-3	Qp > 3	K	P	Lm	Lv	Ls	Cht	Qm	Qp	Qt	F	L	Lt	Q	RF
1	R61	1	94	32	1	46	5	0	71	0	10	41	126	88	214	5	81	169	173	122
2	R63	1	36	46	5	28	6	0	79	0	56	44	82	77	159	6	135	212	115	179
3	R71	1	66	46	8	18	2	0	87	0	19	51	112	77	189	2	106	183	138	157
4	R77	1	62	37	6	15	6	0	98	0	26	49	99	70	169	6	124	194	120	173
5	R80	1	66	49	9	17	3	0	75	0	20	61	115	87	202	3	95	182	141	156
6	R81.5	1	90	64	5	7	1	0	91	0	12	30	154	42	196	1	103	145	166	133
7	S1.5	2	85	54	8	22	4	0	3	0	90	14	139	44	183	4	93	137	169	107
8	S176	2	43	40	2	10	9	2	3	0	135	26	83	38	121	11	138	176	95	164
9	S206	2	54	49	9	14	14	6	3	0	119	19	103	42	145	20	122	164	126	141
10	S218	2	46	33	7	9	3	1	2	0	172	17	79	33	112	4	174	207	95	191
11	S263	2	38	28	2	4	4	0	11	0	179	15	66	21	87	4	190	211	72	205
12	S271	2	47	31	7	14	10	4	3	0	155	19	78	40	118	14	158	198	99	177
13	S315	2	43	36	5	10	8	0	7	0	155	22	79	37	116	8	162	199	94	184
14	S318	2	36	32	6	5	2	0	18	0	159	27	68	38	106	2	177	215	79	204
15	V234	3	36	50	1	17	7	0	28	0	147	26	86	44	130	7	175	219	104	201
16	V242	3	39	49	4	9	3	0	29	0	145	23	88	36	124	3	174	210	101	197
17	V268	3	37	51	1	15	5	0	30	0	139	23	88	39	127	5	169	208	104	192
18	V338	3	36	87	4	16	8	0	29	0	104	22	123	42	165	8	133	175	143	155
19	V430	3	66	106	7	11	10	0	25	0	65	10	172	28	200	10	90	118	190	100
20	V566	3	167	50	7	16	4	0	23	0	18	27	217	50	267	4	41	91	240	68
21	V710	3	171	34	1	11	12	0	33	0	47	9	205	21	226	12	80	101	217	89
22	V836	3	66	104	16	19	15	0	37	0	58	3	170	38	208	15	95	133	205	98
23	V856	3	143	60	6	16	7	0	22	0	24	12	203	34	237	7	46	80	225	58
24	C514	4	79	31	1	21	2	0	13	0	115	30	110	52	162	2	128	180	132	158
25	C533	4	87	45	7	9	19	0	19	0	88	17	132	33	165	19	107	140	148	124
26	C667	4	103	45	9	14	18	0	16	0	92	3	148	26	174	18	108	134	171	111
27	C737	4	172	20	2	14	16	0	10	0	65	9	192	25	217	16	75	100	208	84
28	C911	4	113	40	0	10	6	0	17	0	102	7	153	17	170	6	119	136	163	126
29	C964	4	169	54	6	15	14	1	12	0	30	9	223	30	253	15	42	72	244	51
30	P242	5	138	31	49	25	0	0	0	0	1	38	169	112	281	0	1	113	243	39
31	P254	5	150	21	54	42	4	0	0	0	2	22	171	118	289	4	2	120	267	24
32	P256	5	158	31	21	47	7	0	1	0	0	32	189	100	289	7	1	101	257	33
33	P258	5	177	21	7	37	6	0	0	0	4	42	198	86	284	6	4	90	242	46
34	P284	5	188	18	12	24	4	0	0	0	0	32	206	68	274	4	0	68	242	32
35	P300	5	192	23	4	21	9	0	1	0	0	35	215	60	275	9	1	61	240	36
36	P302	5	194	23	9	14	19	0	1	0	3	28	217	51	268	19	4	55	240	32
37	L410	6	186	73	15	9	9	0	0	0	0	5	259	29	288	9	0	29	283	5
38	L530	6	145	68	10	13	12	0	0	0	1	22	213	45	258	12	1	46	236	23
39	L537	6	111	63	11	24	28	0	0	0	0	28	174	63	237	28	0	63	209	28
40	L549	6	159	89	8	18	6	0	0	0	0	18	248	44	292	6	0	44	274	18
41	L568	6	150	87	14	5	12	0	0	0	0	28	237	47	284	12	0	47	256	28
42	L585	6	213	50	9	7	4	0	0	0	0	10	263	26	289	4	0	26	279	10

Table 3. Average of major and trace elements composition of sandstones and shales from the Ab-Haji Formation (oxides in %, elements in ppm).

Sample location	1	2	2	3	3	4	4	5	6	6
Lithology	Sandstone	Sandstone	Shale	Sandstone	Shale	Sandstone	Shale	Sandstone	Sandstone	Shale
No.	3	5	5	7	4	5	4	7	5	3
SiO_2	79.31	76.86	62.69	70.57	64.51	85.75	65.46	88.16	95.57	64.51
Al_2O_3	11.34	10.66	17.3	8.98	17.79	6.79	17.71	5.51	1.63	17.79
Na_2O	0.13	1.48	0.99	0.22	0.26	0.25	0.3	0.15	0.03	0.26
K_2O	1.91	1.55	3.29	1.4	2.82	1.01	2.88	0.73	0.23	2.82
Fe_2O_3	1.91	4.13	6.22	9.53	4.95	2.4	3.4	1.03	0.71	4.95
MgO	0.47	1	1.66	1.07	1.36	0.56	1.16	0.28	0.06	1.36
CaO	0.18	0.35	0.56	0.29	0.28	0.09	0.49	0.26	0.3	0.28
TiO_2	0.62	0.57	0.88	0.56	0.91	0.47	0.97	0.44	0.14	0.91
P_2O_5	0.05	0.11	0.08	0.1	0.12	0.04	0.07	0.03	0.02	0.12
MnO	0.01	0.02	0.04	0.17	0.06	0.02	0.03	0.01	0.01	0.06
Cr_2O_3	0.02	0.02	0.01	0.02	0.02	0.03	0.02	0.03	0.04	0.02
FeO	0.86	1.86	2.8	4.29	2.23	1.08	1.53	0.46	0.32	2.23
Fe_2O_3*	1.05	2.27	3.42	5.24	2.72	1.32	1.87	0.57	0.39	2.72
Ni	78	33.6	49.8	31.33	47.5	29.2	52.33	38	<20	47.5
Sc	8.33	8	15	7.57	14.25	5	14.5	5	1.67	14.25
Ba	237.33	210.8	405.4	211.57	341.25	131.6	372.5	101.57	36.8	341.25
Be	1.5	1.75	2.6	1.86	2.5	1	4.25	3	<1	2.5
Co	5.13	11.1	18.8	11.47	18.13	10.44	14.73	4.64	2.6	18.13
Cs	3.87	2.02	7.26	2.6	8.08	1.34	8.73	1.59	0.38	8.08
Ga	14.03	12.08	20.94	10.5	22.28	8.02	23	6.44	2.1	22.28
Hf	4.7	8.88	5.18	6.6	7.2	7.96	7.03	7.27	4.94	7.2
Nb	14.97	12.32	17.22	11.91	18.88	10.24	20.18	9.41	3.54	18.88
Rb	73.53	54.56	131.8	55.99	122.43	37.82	132.98	30.04	8.06	122.43
Sn	3	2.2	3.4	1.86	3.5	1.8	4	2	<1	3.5
Sr	68.4	89	145.34	49.34	96.05	42.68	109.43	53.9	44.52	96.05
Ta	0.93	0.82	1.3	0.84	1.38	0.8	1.55	0.66	0.28	1.38
Th	9.7	9.96	16.44	8.81	30.25	8.14	18.43	6.6	2.48	30.25
U	1.83	2.14	2.78	2.07	4.18	1.94	3.63	1.84	0.96	4.18
V	85	70.8	134.2	56	124.5	45.2	140	42	14	124.5
W	1.83	1.74	1.94	1.79	2.3	2.14	2.5	2.19	2.36	2.3
Zr	173.53	340.62	194.26	246.23	247.1	305.02	240.5	278.04	184.88	247.1
Y	18.3	21.62	28.04	26.63	34.55	17.22	31.25	14.87	5.98	34.55
La	28.77	26.36	44.6	28.93	76.73	25.2	48.38	18.63	8.08	76.73
Ce	61.13	54.88	90.86	62.66	155.28	55.18	95.35	39.3	17.04	155.28
Pr	6.78	6.19	10.24	7.05	17.15	5.87	10.64	4.32	1.9	17.15
Nd	24.5	24.34	37.86	26.87	61.05	21.16	38.53	15.84	6.88	61.05
Sm	4.73	4.61	7.08	5.22	11.08	3.97	6.97	2.82	1.38	11.08
Eu	0.86	0.95	1.35	1.11	1.55	0.71	1.37	0.56	0.25	1.55
Gd	3.93	4.55	5.78	5.2	9.69	3.44	6.05	2.64	1.21	9.69
Tb	0.57	0.7	0.92	0.83	1.23	0.52	0.96	0.42	0.18	1.23
Dy	3.38	3.94	5.11	4.65	6.66	3.01	5.35	2.51	1.02	6.66
Ho	0.64	0.73	1.06	0.85	1.16	0.59	1.1	0.5	0.19	1.16
Er	1.95	2.16	3.01	2.39	3.37	1.71	3.22	1.44	0.59	3.37
Tm	0.29	0.33	0.47	0.36	0.52	0.26	0.51	0.22	0.09	0.52
Yb	1.9	2.2	2.99	2.21	3.2	1.67	3.14	1.57	0.6	3.2
Lu	0.29	0.32	0.46	0.34	0.48	0.26	0.51	0.23	0.1	0.48
Mo	1.17	1.26	0.52	1.13	0.48	1.72	0.55	1.66	3.48	0.48
Cu	13.5	21.28	31.28	15.77	26.95	10.7	36.35	7.53	4.42	26.95
Pb	2.7	8.44	12.5	6.36	16.58	4.5	18.8	3.91	2.86	16.58
Zn	143	62.2	87.4	43.57	55.75	37.6	83.75	20.43	3	55.75
Ni	23.8	26.96	45.12	24.54	42.08	23.04	34.1	9.69	7.7	42.08
As	2.7	4.7	4.37	1.6	2.6	2.04	4.8	3.15	1.38	2.6
Cd	<0.1	<0.1	<0.1	<0.1	0.1	<0.1	<0.1	<0.1	<0.1	0.1
Sb	<0.1	<0.1	<0.1	<0.1	<0.1	<0.1	0.2	<0.1	<0.1	<0.1
Bi	0.2	0.17	0.28	0.2	0.28	<0.1	0.23	0.3	<0.1	0.28
Ag	<0.1	<0.1	<0.1	<0.1	<0.1	<0.1	0.1	<0.1	<0.1	<0.1
Au	1.4	1.63	1.2	<0.5	0.7	0.73	2.1	0.95	0.5	0.7
Hg	0.03	<0.01	0.01	0.02	0.04	0.02	0.04	0.03	0.11	0.04
Tl	<0.1	0.1	<0.1	<0.1	0.1	<0.1	<0.1	<0.1	<0.1	0.1
Se	<0.5	<0.5	<0.5	<0.5	<0.5	<0.5	<0.5	<0.5	<0.5	<0.5
LOI	4	3.16	6.2	7.03	6.75	2.56	7.43	3.34	1.3	6.75
Sum	99.92	99.9	99.95	99.92	99.84	99.95	99.91	99.96	100.01	99.84
CIA	83.91	70.24	76.67	82.50	83.78	82.00	83.82	85.50	85.20	78.15

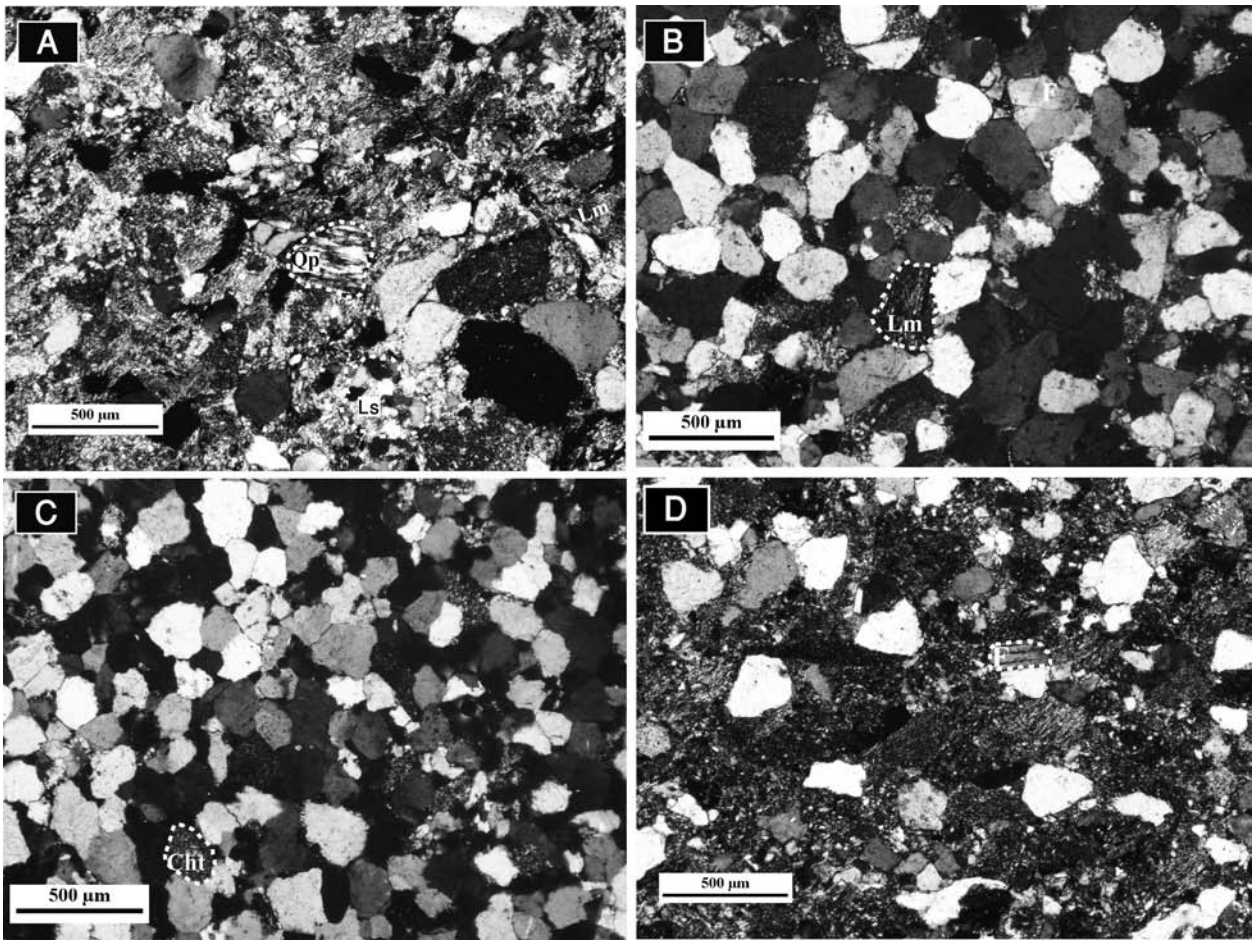

Fig. 6. Thin-section photomicrographs of representative sandstones of the Ab-Haji Formation. A. Polycrystalline quartz grain (Qp) and sedimentary rock fragment (Ls) (sample from section 1). B. Metamorphic rock fragment (slate with slaty cleavage; Lm) and rounded, non-undulose quartz grains in upper right of the photograph (sample from section 3). C. Monocrystalline quartz (Qm) and chert grain (Cht) (sample from section 5). D. Plagioclase (F) grain in an immature litharenite (sample from section 2).

After careful petrographic examination, whole-rock chemical analyses were performed on 32 sandstone and 16 shale samples to obtain analytical data for major, trace and rare earth elements. Analyses were performed by inductively coupled plasma-mass spectrometry (ICP-MS) at ACME Analytical Laboratories, Vancouver, Canada (Table 3).

5. Results

5.1 Sandstone petrography and modal analysis

The following text briefly describes the texture and major grain components of sandstones from the Ab-Haji Formation. Sandstones from the western Tabas Block (sections 1 through 4) are generally moderately sorted, immature and medium- to coarse-grained; individual grains are sub-rounded to rounded. Some samples contain up to 15% of pseudomatrix, derived from deformed soft lithic clasts and altered feldspars (Fig. 6A, B). In contrast, the samples from the eastern Tabas and western Lut blocks (sections 5 and 6) are composed of well sorted, mature to supermature, medium- to fine-grained sandstones devoid of matrix (Fig. 6C). Silica cement is predominant in the sandstones from the eastern Tabas and western Lut blocks whereas calcite, dolomite and iron oxides together with silica cements are more common in the sandstones from the western Tabas Block.

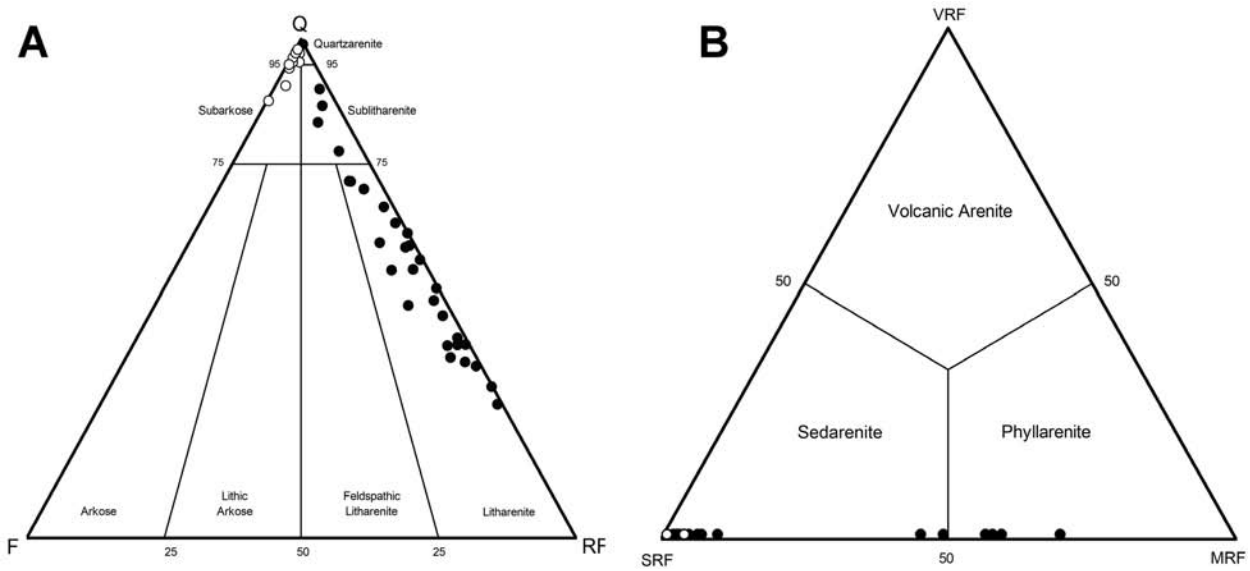

Fig. 7. **A.** and **B.** Mineralogical classification of the sandstones from the Ab-Haji Formation in the Folk (1974) diagram: Q: total quartz; F: feldspar; RF: rock fragment; SRF: sedimentary rock fragment; VRF: volcanic rock fragment; MRF: metamorphic rock fragment. Black circles mark samples from outcrop sections 1-4, white circles from outcrop sections 5-6.

Sandstone framework grains from all localities are mainly quartz and rock fragments as well as subordinate feldspars (Table 2). Quartz is the predominant constituent in all of the sandstones and shows a high Qm/Qp ratio. Rounded, non-undulose quartz is the main quartz grain type (Fig. 6B, C). According to the genetic classification of quartz types (Folk 1974), non-undulose quartz is uncommon in plutonic and metamorphic rocks, whereas mature sedimentary rocks are characterized by high percentages of non-undulose quartz.

Polycrystalline quartz grains commonly include stretched metamorphic quartz with crenulated or granulated boundaries between elongate crystals, showing strong undulose extinction (Fig. 6A).

Sedimentary (Ls) and (meta-) sedimentary (metamorphic, Lm) lithic fragments occur in variable proportions throughout the Ab-Haji sandstones in the western Tabas Block. Volcanic lithics (Lv) are absent.

Sedimentary lithics (Ls) constitute the major rock fragment fraction. They comprise mainly siltstones, shales, sandstones and cherts in the western and southern Tabas Block. In the eastern Tabas and western Lut blocks, only chert has been observed (Fig. 6A, C). (Meta-) sedimentary lithics (low-grade metamorphic, Lm), including slates and phyllites, predominate in the western Tabas Block while being uncommon in sections from the eastern Tabas and western Lut blocks (Fig. 6B). The feldspars are dominated by untwinned orthoclases and subordinate plagioclases (Fig. 6D). K-feldspar grains are typically similar to quartz in grain size but show variable degrees of roundness. The dominant heavy minerals include zircon, epidote, tourmaline and opaque minerals.

Sandstone composition from the Ab-Haji Formation plot in the quartzarenite, quartz-rich sublitharenite and litharenite fields of a QFL ternary plot (Folk 1974) (Fig. 7A, B). Sandstone composition of the western Tabas Block mainly comprise litharenites to quartz-rich sublitharenites, whereas sandstones of the eastern Tabas Block and western Lut Block plot in the quartzarenite field.

5.2 Geochemistry

The geochemical composition of sedimentary rocks results from the complex interaction of several variables, including, source material, weathering, transport, physical sorting and diagenesis (Middleton 1960; Piper 1974; Bhatia 1983; McLennan 1989; Cox et al.

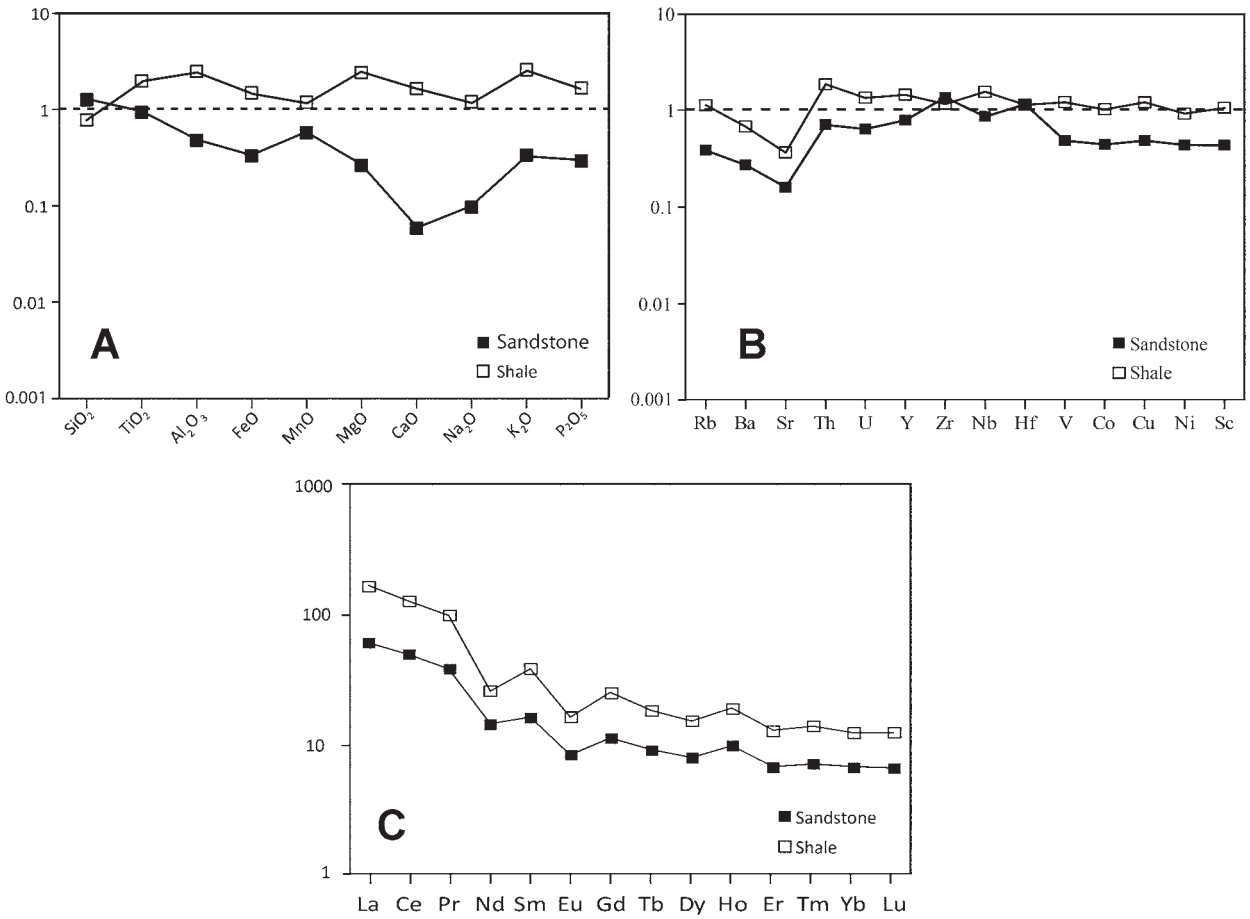

Fig. 8. Spider plot of major (A) and trace (B) element compositions of sandstone and shale samples from the Ab-Haji Formation, normalized against UCC (upper continental crust) values (UCC values after Taylor & McLennan 1985). The trace elements are ordered showing LILE on the left (Rb-U), followed by HFSE on the right (Y-Hf) followed by TEE (V-Sc). C. Average chondrite-normalized Rare Earth Element plots for samples from the Ab-Haji Formation.

1995). The average major and trace element concentrations of the Ab-Haji sandstones (32 samples) and shales (16 samples) are listed in Table 3.

The major element distribution reflects the mineralogy of the studied samples. Petrographic observations show that the sandstones of the Ab-Haji Formation display compositional variations from litharenites through to quartzarenites (see above). This is best depicted by the SiO_2 concentration which range from ~75% in litharenites and quartz-rich sublitharenites to ~94% in quartzarenites. Sandstones are higher in SiO_2 than shales (Table 3) while shales are higher in Al_2O_3, MgO, K_2O, Fe_2O_3 and TiO_2 than sandstones, reflecting the dominance of clay minerals and clay-sized particles (Cardenas et al. 1996; Madhavaraju & Lee 2010). Concentrations of most major elements in the sandstones are generally similar to the mean composition of upper continental crust (UCC) (Taylor & McLennan 1985), except for CaO, Na_2O and K_2O, which consistently yield lower-than-average values (Fig. 8A).

Low concentrations of CaO may either indicate a lack of original carbonate minerals or depletion of Ca during diagenesis. The depletion of Na_2O (~0.45) and K_2O (~1.78) in sandstones can be attributed to a relatively low proportion of Na-rich plagioclase and K-feldspar; this is consistent with the petrographic data.

Shale samples from the Ab-Haji Formation show higher-than-mean upper continental crust (UCC) concentrations of most of the major elements, possibly be-

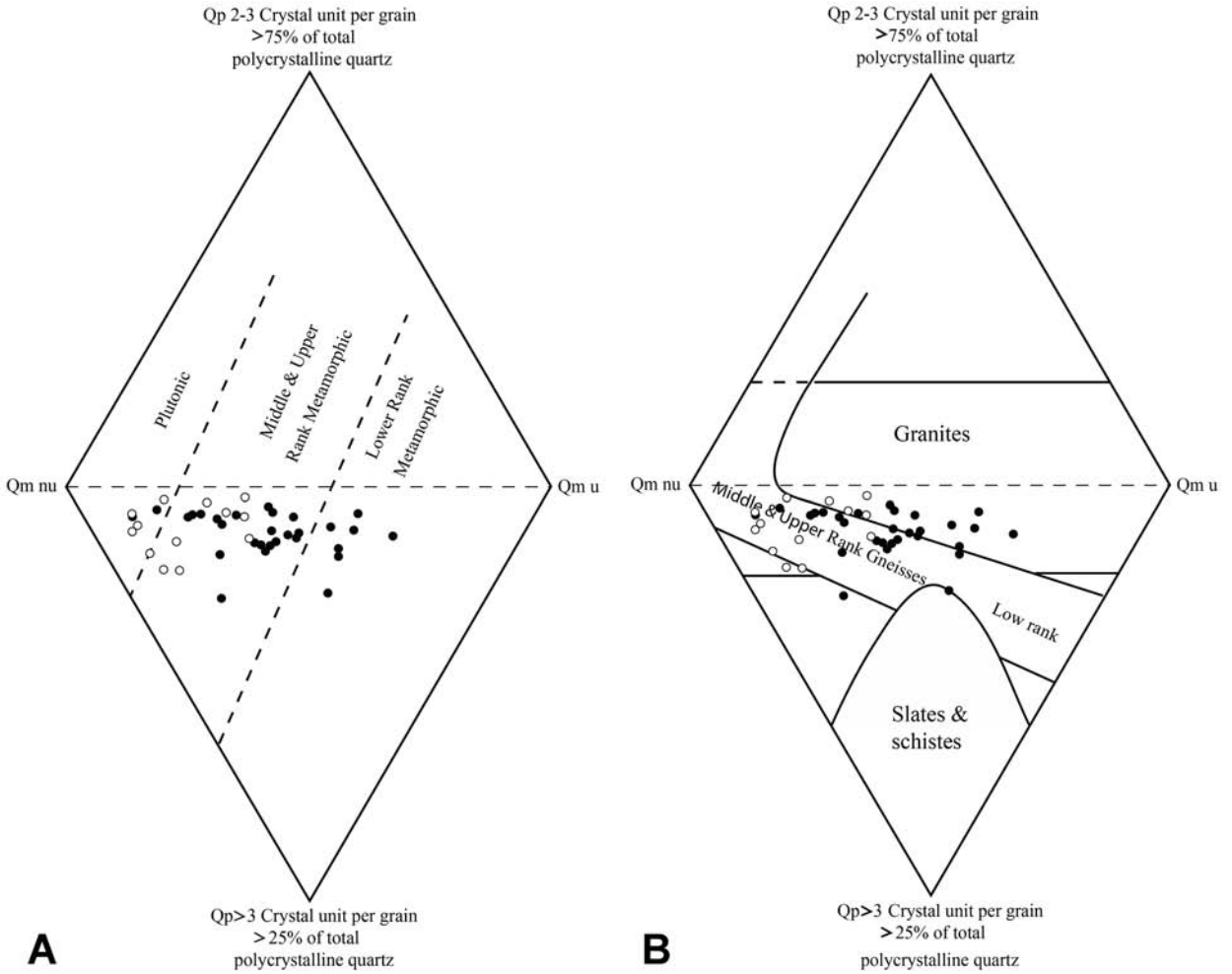

Fig. 9. Quartz grain varieties in the sandstones from the Ab-Haji Formation plotted on the diamond-shaped diagrams after Basu et al. (1975) (A) and Tortosa et al. (1991) (B). Qp: polycrystalline quartz; Qm u: monocrystalline quartz with undulose extinction; Qm nu: monocrystalline quartz with straight extinction. For symbols refer to Fig. 7.

cause Al, Ti, Mg and K are easily absorbed by clays and concentrate in the finer-grained particles (Das et al. 2006). On average, the Ab-Haji shales have slightly lower SiO_2 abundances relative to UCC, possibly due to a quartz dilution effect (Bauluz et al. 2000).

Most trace element values, including large ion lithophile elements (LILE, including Rb, Ba, Sr, Th and U), high field strength elements (HFSE, including Y, Zr, Nb and Hf), transition trace elements (TTE, including V, Co, Cu, Ni and Sc) and rare earth elements (REE) of sandstones and shales from the Ab-Haji Formation are generally similar to UCC values (Fig. 8B). With the exception of Sr, all samples exhibit similar LILE and HFSE abundances relative to UCC (Fig. 8B). Because HFSE elements are enriched in felsic rather than mafic rocks (Bauluz et al. 2000), felsic materials may have predominated in the source area.

TTE in sandstones are also similar to UCC, but are depleted in the shale samples. The chondrite-normalized rare earth element (REE) patterns of the studied samples are characterized by LREE enrichment and fairly flat HREE patterns, similar to old upper con-

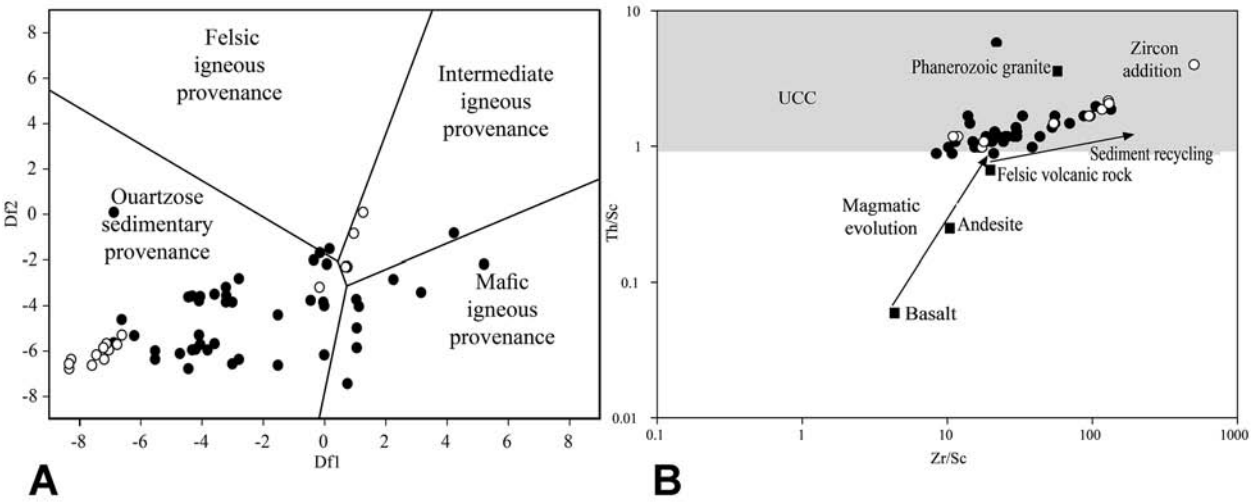

Fig. 10. A. Major element discriminant function diagram of Roser & Korsch (1988) illustrating sedimentary provenance. Discriminant functions include: Discriminant Function 1 = (-1.773.TiO_2) + (0.607.Al_2O_3) + (0.760.Fe_2O_3) + (-1.500.MgO) + (0.616.CaO) + (0.509.Na_2O) + (-1.224.K_2O) + (-9.090); Discriminant Function 2 = (0.445.TiO_2) + (0.070.Al_2O_3) + (-0.250.Fe_2O_3) + (-1.142.MgO) + (0.438.CaO) + (1.475.Na_2O) + (1.426.K_2O) + (-6.861). B. Plot of Th/Sc versus Zr/Sc of Lower Jurassic sandstones from Ab-Haji Formation (modified after (McLennan et al. 1993). Sandstones from the Ab-Haji Formation are enriched in zircon due to sedimentary sorting and recycling (igneous rock averages from Condie 1993); UCC composition after Taylor & McLennan (1985). The lower arrow (compositional trend) define the trend expected in first-cycle sediments due to magmatic evolution from mafic to felsic; upper arrow shows the trend produced by the addition of zircon during sedimentary sorting and recycling. For explanation of symbols, see Fig. 7.

tinental crust (Fig. 8C). The LREE enrichment and the almost flat HREE pattern may indicate a cratonic source rock with felsic plutonic and (meta-) sedimentary components (Das et al. 2006).

6. Discussion

6.1 Provenance

6.1.1 Petrography

Sandstone petrography is widely considered to be a powerful tool for determining the origin of ancient clastic deposits (Blatt 1967; Dickinson 1970; Pettijohn et al. 1972; Garzanti & Vezzoli 2003; Garzanti et al. 2007). When plotted in a double-triangular diagram (Basu et al. 1975), sandstone point count data of the Ab-Haji Formation mostly suggest a mix of medium- to high-grade metamorphic and plutonic source rocks (Fig. 9A-B). Low-grade metamorphic components do not appear in this diagram (Fig. 9B). However, Blatt & Christie (1963) have shown empirically that undulose and polycrystalline quartz is less stable than non-undulose and monocrystalline quartz and will break down to produce monocrystalline quartz grains. Consequently, the longer the effective residence time of a population of quartz in the "sedimentary mill", the more the position of that population will move towards the non-undulose quartz pole of the diagrams (Fig. 9A-B).

Stretched polycrystalline quartz grains with sutured intercrystal boundaries are common in samples from sections 1-4 (Fig. 6A), suggesting they were derived from low- to medium-grade metamorphic rocks (Basu et al. 1975). In contrast, monocrystalline, non-undulose quartz is the dominant quartz type in sections 5 and 6 (Fig. 6C), indicating a granitoid source rock (Suttner et al. 1981). However, the rounded to well-rounded quartz grains (Fig. 6B-C) along with chert and siltstone fragments in samples from all six sections indicate that quartz-rich sedimentary rocks also should be considered as significant contributors to sandstone composition.

The composition of sandstones from the Ab-Haji Formation suggests several sources most probably the Precambrian and Ordovician–Triassic sedimentary,

low-, middle- to upper-rank metamorphic and plutonic rocks of the Yazd Block as well as Carboniferous–Triassic sedimentary rocks from the eastern margin of the Tabas Block (see below).

6.1.2 Geochemistry

In order to use major elements for provenance interpretations, we considered the discriminant functions of Roser & Korsch (1988), which use Al_2O_3, TiO_2, Fe_2O_3*, MgO, CaO, Na_2O and K_2O contents as variables. In this diagram (Fig. 10A), the majority of the Ab-Haji Formation sandstone and shale samples plot in the quartzose sedimentary provenance field and suggests that the sediments were of quartzose recycled origin.

Trace element patterns can be used to determine the source of the sediments and provide useful information about the provenance of sedimentary rocks (e.g., Cullers 1988; Cullers 2000; von Eynatten et al. 2003) because mafic and felsic source rocks differ significantly in specific indicator ratios. Sc and Th are transferred quantitatively from source to sediment; hence, its ratio can be used to monitor the average compositional variation of source rocks (McLennan et al. 1993). Zr/Sc monitors zircon enrichment due to sedimentary sorting and recycling. When Th/Sc is plotted in a Zr/Sc - Th/Sc diagram (Fig. 10B), high Zr/Sc ratios support a recycled source rock provenance for all sandstone and shale samples of the Ab-Haji Formation.

6.2 Tectonic setting

6.2.1 Petrography

The majority of the sandstone samples from the Ab-Haji Formation plot in the recycled-orogen field of a standard ternary QtFL diagram (Dickinson & Suczek 1979) (Fig. 11A). Some rare samples plot in the craton-interior field.

Variations in sedimentary rock fragments as well as low-grade metamorphic rock fragments from sections 1-4 suggest that the grains were sourced from a recycled orogen (Fig. 11A). Within recycled orogens, sediment sources are predominantly sedimentary rocks derived from tectonic settings in which stratified rocks are deformed, uplifted and eroded (Dickinson & Suczek 1979; Dickinson 1985). In contrast, sandstones plotting in the craton-interior field are usually mature or supermature because they are derived from relatively low-lying granitoid and gneissic sources, supplemented by recycled sands from associated platform or passive margin basins and may be subjected to long-term weathering (Dickinson et al. 1983). In a QmFLt diagram (Dickinson et al. 1983; Critelli et al. 2002), samples from the Ab-Haji Formation fall principally within the craton-interior, recycled-orogen and transitional-recycled fields (Fig. 11B). The sandstones of the Ab-Haji Formation of the eastern Tabas and western Lut blocks (sections 5-6) plot in the craton-interior field while the western Tabas Block sandstones from sections 1-4 include samples that plot in the recycled-orogen and transitional-recycled fields. Modal analysis and texture indicate that the latter sandstones are immature, suggesting limited transport. The position within the diagrams near the quartz pole (i.e. for sandstones of sections 5-6) would suggest a considerable transport distance, a high degree of sedimentary recycling, and/or highly abrasive transport processes (Folk 1951; Cox et al. 1995). Not all of these factors may have contributed to the petrographic composition of the Ab-Haji Formation, but – in the absence of evidence for aeolian transport or extensive fluvial transport – intensive sediment recycling of older sedimentary rocks in a continental interior setting is likely to have been the main mechanism of mineralogical maturation. Sediment recycling resulted in a shift of compositional data towards a cratonic provenance and a passive-margin tectonic setting, especially for the samples from the eastern Tabas and western Lut blocks. In support of this concept, Hulka & Heubeck (2010) showed that the craton-interior characteristics of some sandstone samples may result from the recycling of older formations of continental sedimentary petrographic character. Uplifted older mature sedimentary material is indeed widely available in Central Iran and thus likely the principal source for the Ab-Haji Formation across the study area: The Permian-age mature and recycled quartzarenites of the Yazd Block (Hosseini-Barzi & Shadana 2010) and siliciclastic intercalations in the Nayband Formation (Fürsich et al. 2005a) and/or the Carboniferous–Permian Sardar Group (Leven et al. 2006) of the Shotori Mountains probably provided source material for the Ab-Haji Formation during the Early Jurassic.

6.2.2 Geochemistry

The major element geochemistry of the sandstone and shale samples from the Ab-Haji Formation (Table 3) were analysed using ternary plots to characterize the tectonic setting as proposed by Kroonenberg (1994). This diagram suggests that the samples were deposited in a passive continental margin (Fig. 12A).

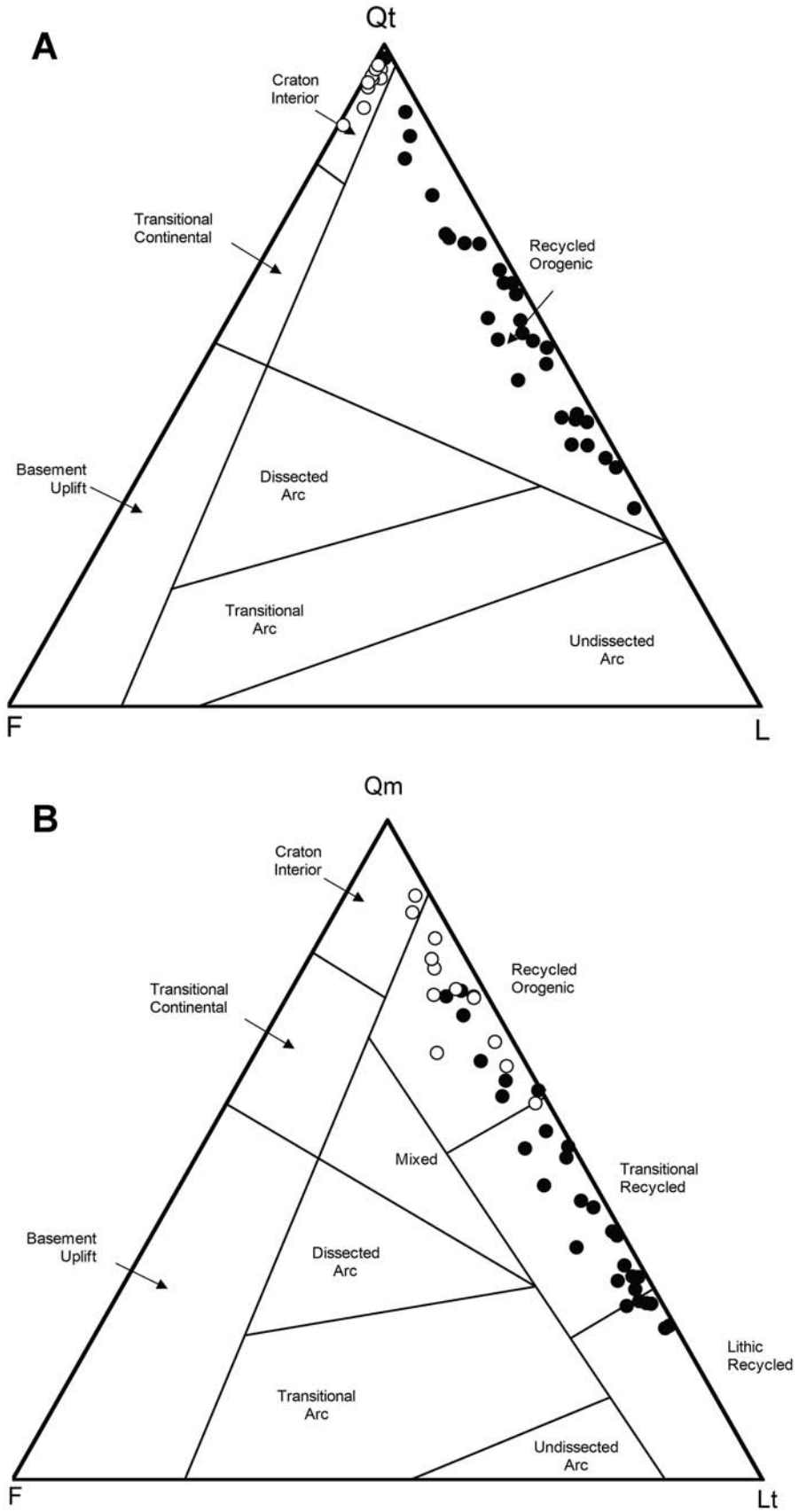

Fig. 11. QtFL (A) and QmFLt (B) plots for tectonic provenance of sandstones from the Ab-Haji Formation. Provenance fields after Dickinson & Suczek (1979). For symbols, refer to Fig. 7.

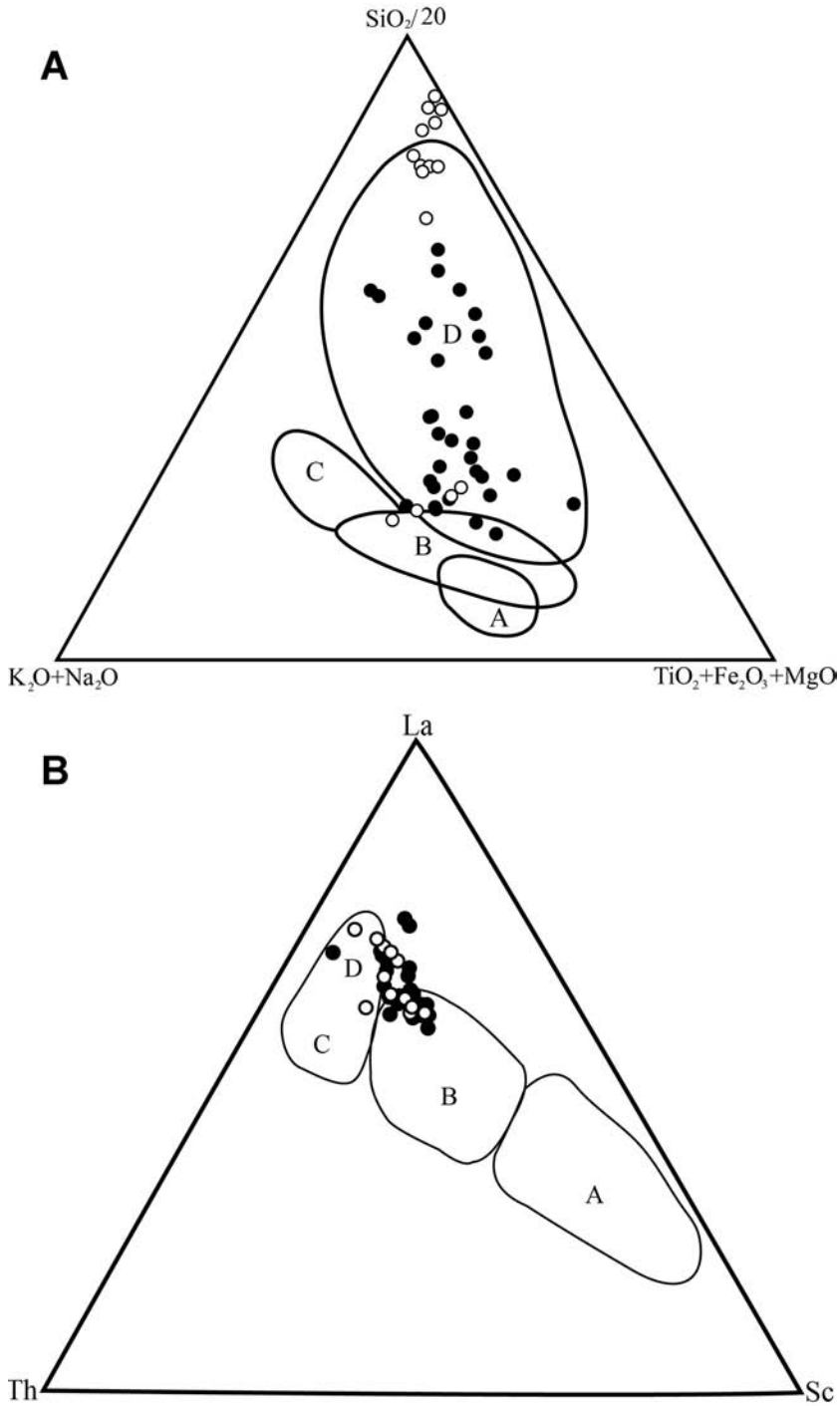

Fig. 12. A. Plot of the major element composition of Ab-Haji Formation sandstone and shale samples on the tectonic setting discrimination diagram of Kroonenberg (1994). B. Trace element composition of sandstone and shale samples from the Ab-Haji Formation on the ternary tectonic setting diagram of Bhatia & Crook (1986). See text for details. Legend: A: oceanic island arc; B: continental island arc; C: active continental margin; D: passive continental margin. For symbols, refer to Fig. 7.

Trace elements, particularly those with relatively low mobility and low residence times in seawater, such as Th, Sc, Ti, Nb and Zr are transferred quantitatively into clastic sediments during primary weath-

ering and transportation and are thus useful tools for the discrimination of provenance and tectonic setting (Taylor & McLennan 1985; Bhatia & Crook 1986; McLennan 1989; McLennan & Taylor 1991). On the La-Th-Sc diagram of Bhatia & Crook (1986) (Fig. 12B), the Ab-Haji Formation samples mostly plot in the passive-margin field. The same geochemical data, plotted in the diagram presented by Cullers (1994), fall in a mixed field indicating that the Ab-Haji sediments were derived from a mixed sedimentary or (meta-)sedimentary source. The distinctive depletion in Sr in both sandstone and shale samples (Fig. 8B) also suggests a recycled-orogen or passive margin setting (e.g., Najafzadeh et al. 2010).

These indications are, however in contrast to the regional geodynamic setting of the study area which is more consistent with a broad back-arc (or retro-arc) basin (Wilmsen et al. 2009b). These apparent inconsistencies need to be addressed.

A passive-margin setting is unlikely and can be excluded because the onset of Neotethys subduction at the southwestern margin of the Iran Plate in the Norian–Rhaetian is well established (subduction-related magmatism in the Sanandaj-Sirjan Zone; Arvin et al. 2007; Wilmsen et al. 2009b). It persisted with varying intensity throughout the Mesozoic and Cenozoic (e.g., Chiu et al. 2013). Palaeogeographic reconstructions (Barrier & Vrielynck 2008) indicate only limited volcanic activity at the active margin during the Early Jurassic, supported by recent studies from the Urumieh-Dokhtar magmatic arc and the Sanandaj-Sirjan structural zone in Iran (Chiu et al. 2013). Behind the arc, a broad (retro-arc) zone of subduction-related extension with block-faulting produced an array of swells and basins on the Iran Plate. Major extensional zones were situated in the Alborz (Fürsich et al. 2005b) and in the South Caspian area (Brunet et al. 2003). The exposed zones (such as the Shotori Swell and the Yazd Block) yielded sediments of recycled-orogen character (strata consolidated by the Cimmerian orogeny); in addition, the significant distance to the poorly active magmatic arc limited the input of volcanic components. The common asymmetric geometry of continental back-arc basins may also have reduced magmatic components in the Ab-Haji Formation. This type of basin commonly shows a steep, thrust-faulted arcward margin and a more gently-dipping, block-faulted inner craton margin (Einsele 2000). The Tabas and Yazd blocks are located on this inner margin so that cratonic sediment sources predominated there (Einsele 2000). Possibly, the shallow angle of Neotethys subduction beneath southwest Iran (Ghasemi & Talbot 2006) caused both the limited volcanic activity in the arc and the very broad extensional retro-arc zone.

6.3 Source area weathering

Point count data from sandstones of the the Ab-Haji Formation plot in the Weltje et al. (1998) diagram in the arrow-shaped field (Fig. 13A), representing a mixture of metamorphic, sedimentary and plutonic source rocks. According to the Weathering Index (WI = c * r) introduced by (Grantham & Velbel 1988), almost all sandstones sample plot into the WI field 4, indicating a high degree of weathering under humid climate conditions (Fig. 13B). In addition, the sandstones of the Ab-Haji Formation suggest semi-humid to humid climate conditions when plotted in the bivariate diagram of (Suttner & Dutta 1986) (Fig. 13C).

The degree of weathering in source rocks can be estimated by various chemical indices relying on their major element compositions. A widely used example is the CIA index (Chemical Index of Alteration, Nesbitt & Young 1982), which is based on the assumption that the prevailing processes during chemical weathering are feldspar degradation and formation of clay minerals. The CIA, therefore, is potentially a very useful index to characterize the degree of weathering of the sediment source and in terms of variable source terrains. Worldwide average shale CIA values range between about 70 and 75; fresh granites give values of around 50 (Visser & Young 1990); extreme weathering may produce values approaching 100. The CIA (calculated as CIA = $100 \times Al_2O_3/Al_2O_3+CaO^*+Na_2O + K_2O$) of sandstone and shale samples from the Ab-Haji Formation show that weathering resulted in a relative loss of Na, Ca and K, and in an increase in Al (Table 3; oxides are expressed as molar proportions and CaO* represents the Ca in silicate fractions only). The samples have CIA values between 69 and 89, indicative of moderate to intense weathering of first-cycle sediment, or alternatively, recycling. The A-CN-K ternary diagram (Nesbitt & Young 1984) can also be used to constrain the weathering condition in the source area. The major sandstone and shale samples plot close to the top axes and the Al_2O_3-K_2O boundary (Fig. 14). Therefore, the positions of the samples in the A-CN-K diagram, as well as their CIA values, are consistent with moderate to intense weathering conditions or recycling processes. Our results thus suggest that semi-humid to humid climatic condition along with recycling of older sedimentary successions resulted in

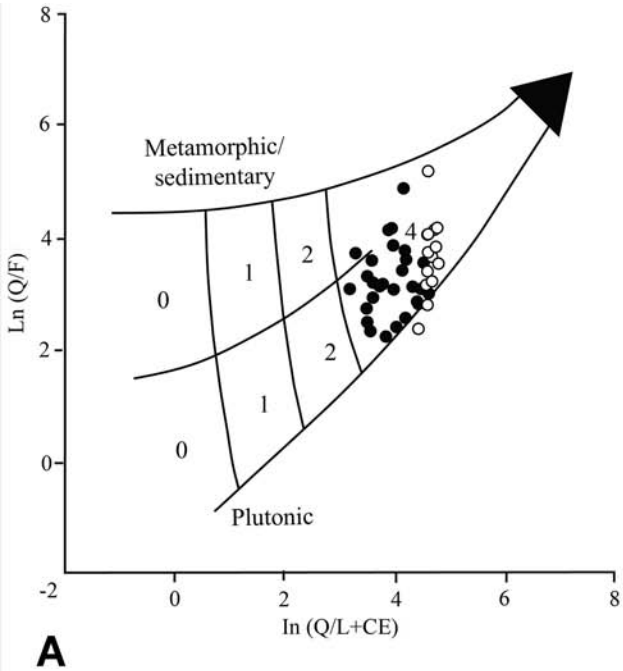

Semi-quantitative weathering index (wi=c*r) (Weltje, 1994)		Relief (r) high, mountains 0	moderate, hills 1	low, plains 2
Climate (c) (Semi-)arid, mediterrane	0	0	0	0
temperate, subhumid	1	0	1	2
tropical, humid	2	0	2	4

B

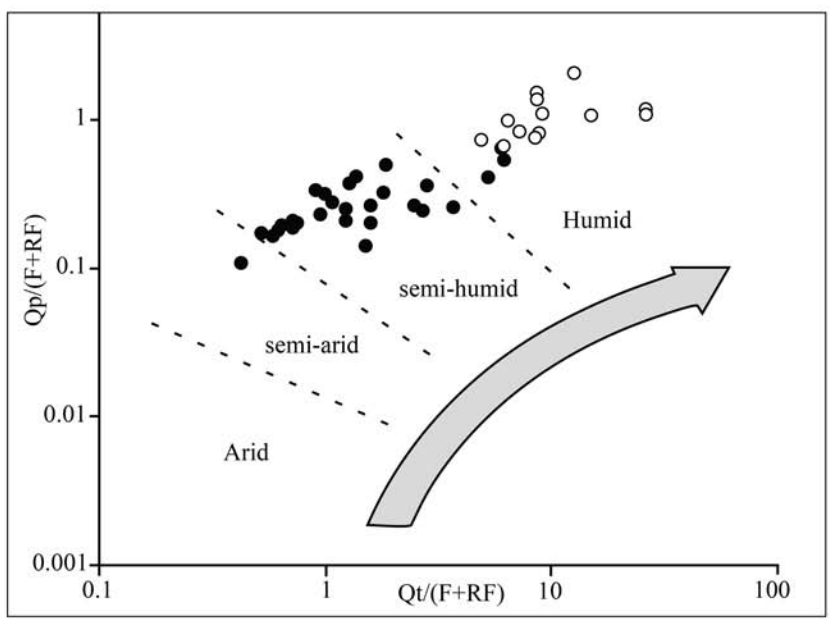

Fig. 13. Climatic conditions and their effect on the composition of sandstones from the Ab-Haji Formation in the log-ratio plot (A) after Weltje et al. (1998). Q: quartz, F: feldspar, RF: rock fragments. CE: carbonate clasts. Fields 1-4 refer to the semi-quantitative weathering indices. B. Semi-quantitative weathering index defined on the basis of relief and climate (after Grantham & Velbel 1988). C. Bivariate plot after Suttner & Dutta (1986) and Johnson & Winter (1999). Qt: total quartz, F: feldspar, RF: rock fragments, Qp: polycrystalline quartz. For symbols, refer to Fig. 7.

a high degree of weathering (WI = 4), indicating low relief and with a humid climate. The abundant coal deposits that developed during the Early Jurassic in Iran are consistent with the climatic conditions inferred

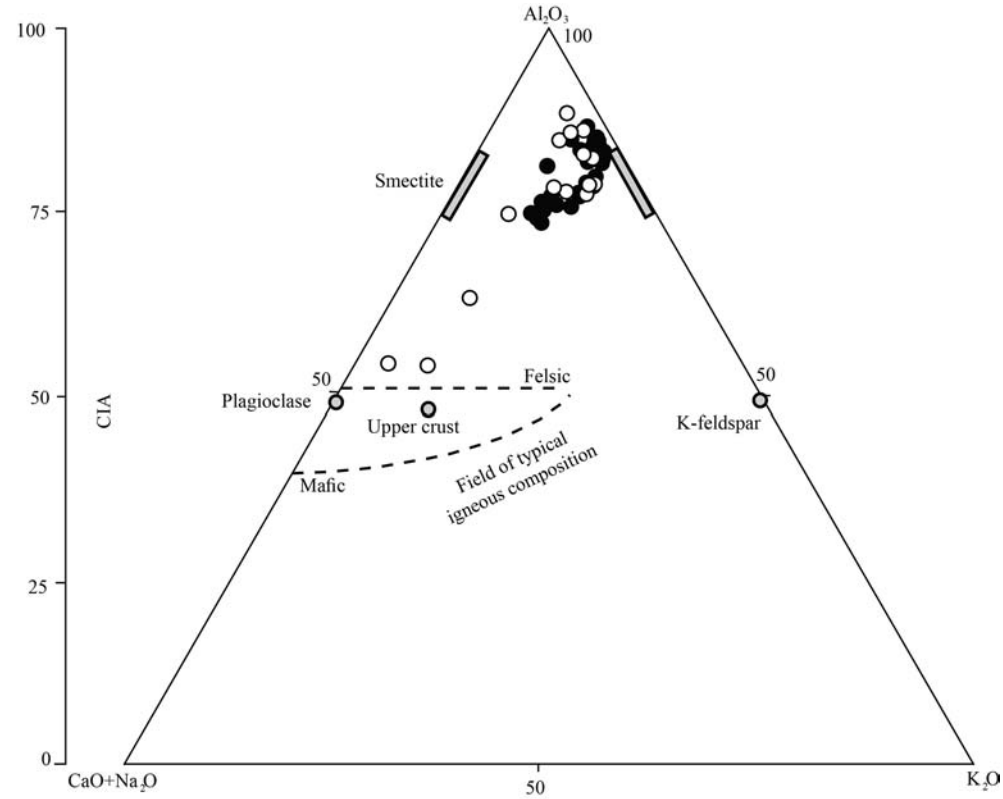

Fig. 14. Al_2O_3 - CaO + Na_2O - K_2O ternary diagram (Nesbitt & Young 1984) showing the high chemical index of alteration (CIA) values of sandstones and shales from the Ab-Haji Formation. For symbols, refer to Fig. 7.

from WI and CIA, although the paleogeographic position of Iran has been reconstructed in somewhat higher palaeo-latitudes than expected (warm-temperate palaeolatitude of ca. 40°-45°N; Thierry 2000). However, the warm climate of the Early Jurassic (e.g., Chandler et al. 1992) may have resulted in a poleward expansion of humid sub-tropical climates.

6.4 Potential source area and paleogeographic implications

A reconstruction of the palaeogeography of the CEIM during the Early Jurassic requires knowledge of the spatial and temporal sedimentation pattern of the Ab-Haji Formation. The well-constrained distribution of the Ab-Haji Formation is explained in an array of extensional tilted blocks (Salehi 2013; Salehi et al. subm.). This tectonic model explains the thickness variations and the rapid E-W facies changes of the Ab-Haji Formation as well as the orientation of areas of non-sedimentation/erosion and the position of the source areas. Extensional tectonic pulses were documented in east-central Iran during the Late Triassic to Late Jurassic (Fürsich et al. 2003; Seyed-Emami et al. 2004b; Fürsich et al. 2005a; Wilmsen et al. 2010; Cifelli et al. 2013). The extensional pulse in the Early Jurassic resulted in block faulting with regional differences in subsidence and synsedimentary block movements that produced basins separated by uplifts. During this time, the Tabas Block was tilted towards the west so that its uplifted margin formed the Shotori Swell, along the trend of the present-day Shotori Mountains (Figs. 2C, 15). The crest of this tilted block was subaerially exposed and became eroded. A similar source area setting is thought to have delivered syntectonic siliciclastics of the Sikhor Formation during the Callovian across the Nayband Fault at the eastern margin of the Tabas Block (Fürsich et al. 2003) and

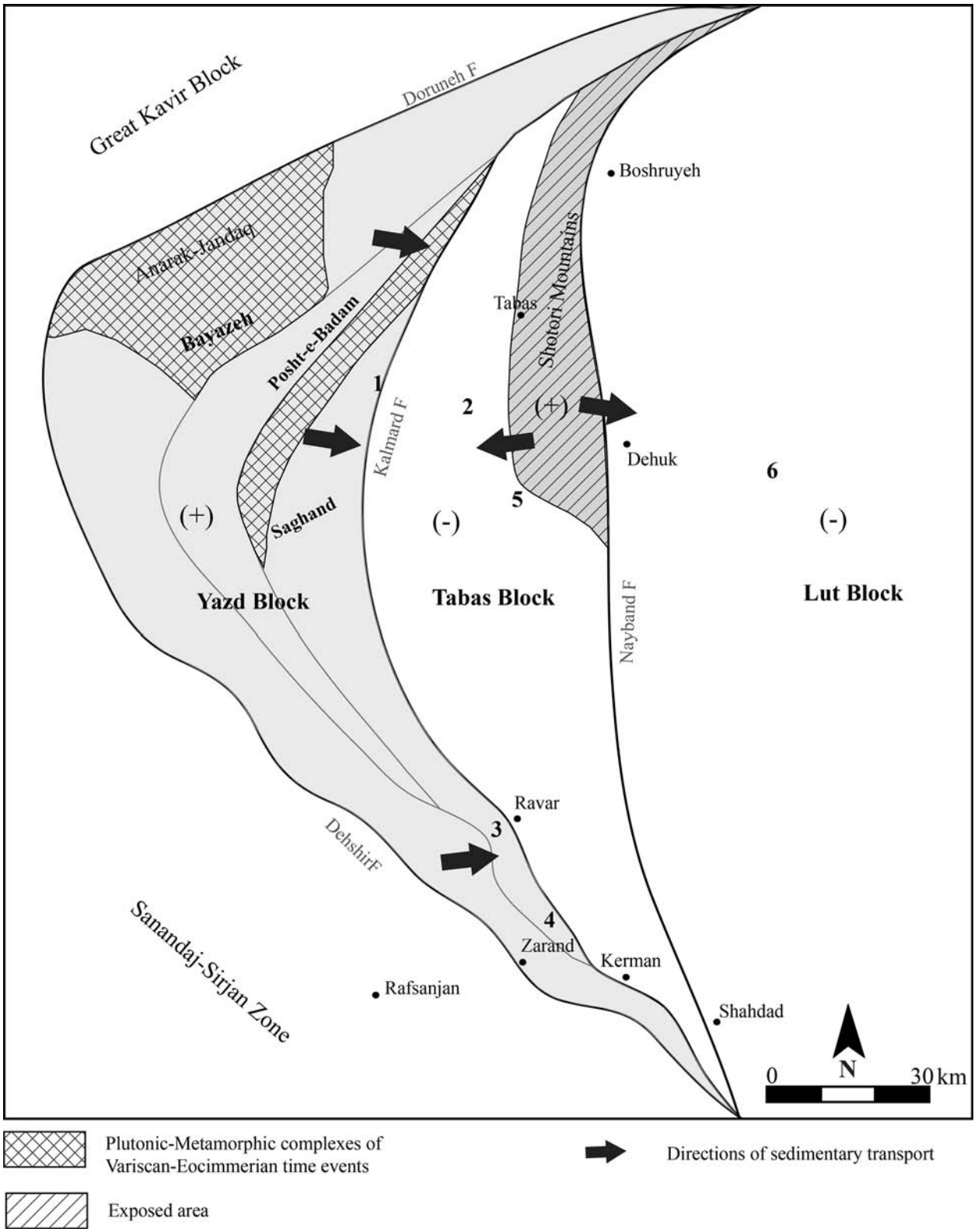

Fig. 15. Potential source area and sediment transport directions for the Ab-Haji Formation in east-central Iran during the Early Jurassic. Gray areas marked by (+) display the assumed uplifted source area while areas marked by (-) indicate zones of subsidence. Blocks and block-bounding faults modified from Wilmsen et al. (2009b)

the thick Nayband Formation on the eastern margin of the Tabas Block (Fürsich et al. 2005a).

There is evidence for synsedimentary exposure and erosion at several localities in the southern Shotori Mountains (Fig. 1B) during the early Jurassic, suggesting a major hiatus and one or several phases of uplift and erosion of the Shotori High (Fürsich et al. 2009b). The Shotori High was also a significant topographic feature during the Late Cretaceous (Wilmsen et al. 2005).

The thickness variations and facies changes in the Ab-Haji Formation follow the pattern of basement uplift and erosion of tilted fault blocks of east-central Iran (Salehi 2013, Salehi et al. subm.). The Ab-Haji Formation is absent from the central Shotori Mountains (Wilmsen et al. 2009a), but appears towards the west at Parvadeh (Section 5), where it is 75 m thick, comprising mainly fluvial and coastal-plain strata. At this locality, the east-west trending fluvial channels of the formation cut erosively into the underlying fine-grained siliciclastic sediments of the Nayband Formation that, along with the well-developed channel facies and the poor development of the fine-grained flood plain deposits, suggest a depositional setting comprising low-sinuosity rivers with a preferred sediment transport direction towards the west-dipping tilted Tabas Block (Salehi 2013; Salehi et al. subm.) (Fig. 15).

At Kuh-e-Shisui on the Lut Block (in the easternmost part of the study area; section 6), the Ab-Haji Formation reappears. Here it consists of c. 210 m of shallow siliciclastic shelf deposits, prodelta sediments and stacked delta-front sandstones with clear evidence of eastward progradation (Salehi 2013; Salehi et al. subm.). Based on the thickness variations, facies changes and evidence of the synsedimentary removal of strata, the siliciclastic rocks of the Ab-Haji Formation in the northeastern Tabas and western Lut blocks were mainly derived from the exposed pre-existing sedimentary successions on the Shotori Swell of the eastern Tabas Block.

The pattern of local erosion on the Yazd Block extending as far down as the Lower Palaeozoic strata during the Middle to Late Triassic (Eo-Cimmerian orogeny) supports a model of basement uplift and erosion of tilted fault blocks (Bagheri & Stampfli 2008). The Ab-Haji Formation overlies Permian strata with a significant stratigraphic gap at section 1 where it is only 82 m thick and composed of shallow-marine sandstone and deltaic facies that prograde eastward. The formation rapidly thickens towards the east and grades equally rapidly into mud-dominated fluvial-plain and thin coastal-plain deposits at section 2 where it is 347 m thick. In the southern Tabas Block (Ravar-Zarand area), the Ab-Haji Formation (section 3-4) shows similar thickness and facies changes as in sections 1 and 2 (Salehi 2013; Salehi et al. subm.). Thus, the Yazd Block may have been a likely source for the siliciclastic rocks along the western margin of the Tabas Block on stratigraphic grounds (Fig. 15) while the presented petrographic and geochemical evidence would also suggest that the pre-Jurassic plutonic, metamorphic and sedimentary rocks of the same block may have provided source material. Subsequently, the plutonic-metamorphic rocks of the Bayazeh and Sagand areas as well as Posht-e-Badam and Chapedony complexes of the Yazd Block have been considered as potential source rocks for Middle to Upper Jurassic strata of the southern Tabas Block (Zamani-Pedram 2011) (Fig. 15).

In support of this hypothesis it should be noted that, low-grade metamorphic (Lm) and sedimentary grains (Ls) are common in sandstones of the Ab-Haji Formation at the western margin of the Tabas Block (Fig. 6A, B; sections 1-4) (Salehi 2012; Shadan & Hosseini-Barzi 2013), but Lm-type grains are not observed in sandstones on the eastern margin of the Tabas (section 5) or Lut blocks (section 6; Fig. 6 C). Therefore, low-grade metamorphic and sedimentary rocks were likely sources for the siliciclastic sediments of the Ab-Haji Formation yielding a mixed recycled provenance from the tilted Yazd Block to the western and southern Tabas Block (Fig. 15). The same source area in the west has been assumed for the subordinate siliciclastic material occurring in the Callovian–Lower Kimmeridgian Kamar-e-Mehdi Formation of the western Tabas Block (Wilmsen et al. 2010).

Shadan & Hosseini-Barzi (2013) considered the displacement of intrabasinal faults (basement fault) and exposure of supracrustal successions (fold-and-thrust belt) due to Eo-Cimmerian orogenic phase related to the central-Iran – Eurasia continental collision at the end of the Triassic as the main mechanisms for supplying sediment to the Ab-Haji Basin. However, Wilmsen et al. (2009a), Salehi (2013) and Salehi et al. (subm.) have suggested that initial plate coupling between the Iran and Turan plates in northern and northeastern Iran in the early Late Triassic (Eo-Cimmerian event) was followed by peripheral foreland sedimentation in the area of the present-day Alborz Mountains. Subsequently, the main Cimmerian uplift phase (due to slab break-off) occurred near the Triassic–Jurassic boundary, resulting in the termination of marine sedimentation as well as non-deposition or erosion, source-area

rejuvenation, and a distinct increase in grain size in the sediments which were deposited in northern and central Iran. This tectonic event also created relief in east-central Iran (Yazd and Tabas blocks) and was followed by a period of extensional tectonics in a retro-arc setting related to the onset of Neotethys subduction below the Iran Plate from the south/southwest (e.g., Arvin et al. 2007; Barrier & Vrielynck 2008). This general geodynamic setting is strongly supported by facies analysis of the Ab-Haji Formation across a large area of east-central Iran (Salehi 2013; Salehi et al. subm.). Our data thus do not support a peripheral foreland basin setting as suggested by Shadan & Hosseini-Barzi (2013), based on their petrographic and geochemical analyses of a single section of the Ab-Haji Formation from the southern Tabas Block.

7. Conclusions

1. The Ab-Haji Formation is a siliciclastic unit of the Shemshak Group between underlying fine-grained sandstones and siltstones of the Nayband Formation and carbonates of the overlying Badamu Formation. The formation is characterized by quartzolithic and quartzose sand- and siltstones and minor coal seams.
2. Sandstone modal analysis shows that the sandstones of this formation on the western and southern Tabas Block consist of immature litharenites to sublitharenites with predominant sedimentary and low-grade metamorphic grains, while the sandstones of the eastern Tabas and western Lut blocks consist of mature quartzarenites.
3. Sandstone and shale geochemistry suggests that most major and trace element values are similar to mean upper-continental-crust values and indicate felsic and (meta-) sedimentary sources.
4. Modal analysis of sandstones and geochemistry of sandstones and shales suggest a derivation from plutonic, metamorphic and quartzose sedimentary source rocks within a recycled-orogen tectonic setting for the western and southern Tabas Block and a cratonic tectonic setting for the eastern Tabas and western Lut blocks.
5. The distribution of major and trace elements in discrimination diagrams suggests that the provenance of the Ab-Haji Formation is consistent with a mixed recycled source and was deposited in a passive-margin tectonic setting.
6. Weathering indices indicate intensive recycling and humid climate favoring profound chemical weathering of the source area and producing compositionally mature sandstones. These processes modified the plotted position of sandstones in tectonic ternary QtFL and QmFLt diagrams to plot in craton-interior and passive-margin fields.
7. The erosion of uplifted pre-Jurassic mature sedimentary strata and low-grade metamorphic rocks exposed on tilted fault blocks within an extensional continental retro-arc basin were likely the main sources for Ab-Haji strata. Palaeogeographic reconstructions and sandstone petrography suggest that the siliciclastic sediments of Ab-Haji Formation were likely derived from the Yazd Block in the west and from the Shotori Swell on the eastern margin of the Tabas Block.
8. The lack of volcanic lithic grains is explained by the significant distance between the inferred volcanic arc at the eastern margin of the Lut Block and the Ab-Haji Basin, by low volcanic activity of this arc during the Early Jurassic, by a high degree of sedimentary recycling and by intensive chemical weathering in the source area.

Acknowledgements

This research represents part of the senior author's Ph.D. thesis and was supported by the Department of Geology, Ferdowsi University of Mashhad, Iran. Point counting was done at the Department of Geosciences, Freie Universität Berlin. We thank Mrs. A. Giribaldi for expert thin section preparation and Mr. M. Jafarzadeh for help with the analytical procedures. E. Zamanian is thanked for assistance in several field work campaigns. Contructive review by anonymous reviewer as well as the editorial work of Prof. Tom McCann are gratefully acknowledged.

References

Aghanabati, S.A. (1975): Etude geologique de la region de Kalmard (W. Tabas). Stratigraphie et tectonique. – Geological Survey of Iran, Report, **53**: 239 pp.

Alavi, M., Vaziri, H., Seyed-Emami, K. & Lasemi, Y. (1997): The Triassic and associated rocks of the Nakhlak and Aghdarband areas in central and northeastern Iran as remnants of the southern Turanian active continental margin. – Geological Society of America Bulletins, **109**: 1563-1575.

Alikhasi, A. (2008): Depositional Environment and Diagenesis of the Ab-e-Haji Formation in Two Outcrop Sections, Sartakht-Shotoran and Cheshme-Bakhshi, Tabas. – 192 pp., M.Sc., University of Shahid Beheshti, Tehran, Iran [in Persian].

Alizadeh, B., Alipour, M., Hosseini, H. & Jahangard, A. (2011): Paleoenvironmental reconstruction using biological markers for the Upper Triassic-Middle Jurassic sedimentary succession in Tabas Basin, central Iran. – Organic Geochemistry, **42**: 431-437.

Arvin, M., Pan, Y., Dargahi, S., Malekizadeh, A. & Ba-

BAEI, A. (2007): Petrochemistry of the Siah-Kuh granitoid stock southwest of Kerman, Iran: Implications for initiation of Neotethys subduction. – Journal of Asian Earth Sciences, **30**: 474-489.

BAGHERI, S. & STAMPFLI, G.M. (2008): The Anarak, Jandaq and Posht-e-Badam metamorphic complexes in central Iran: New geological data, relationships and tectonic implications. – Tectonophysics, **451**: 123-155.

BALINI, M., NICORA, A., BERRA, F., GARZANTI, E., LEVERA, M., MATTEI, M., MUTTONI, G., ZANCHI, A., BOLLATI, I., LARGHI, C., ZANCHETTA, S., SALAMATI, R. & MOSSAVVARI, F. (2009): Triassic stratigraphic succession of Nakhlak (Central Iran), a record from an active margin. – In: BRUNET, M.-F., WILMSEN, M. &GRANATH, J.W. (Eds.): South Caspian to Central Iran Basins: 287-321; United Kingdom (Geological Society of London Special Publications).

BARRIER, E. & VRIELYNCK, B. (2008): Map 2: Middle Toarcian (183.0-175.6 Ma). – In: BARRIER, E. & VRIELYNCK, B. (Eds.): Palaeotectonic maps of the Middle East – tectono-sedimentary–palinsspastic maps from the Late Norian to Pliocene. Paris (Commission for the Geological Map of the World; CGMW / CCGM).

BASU, A., YOUNG, S., SUTTNER, L., JAMES, W. & MACK, G.H. (1975): Re-evaluation of the use of undulatory extinction and crystallinity in detrital quartz for provenance interpretation. – Journal of Sedimentary Petrology, **45**: 873-882.

BAULUZ, B., MAYAYO, M.J., FERNANDEZ-NIETO, C. & GONZALEZ LOPEZ, J.M. (2000): Geochemistry of Precambrian and Paleozoic siliciclastic rocks from the Iberian Range (NE Spain): implications for source-area weathering, sorting, provenance, and tectonic setting. – Chemical Geology, **168**: 135-150.

BESSE, J., TORCQ, F., GALLET, Y., RICOU, L.E., KRYSTYN, L. & SAIDI, A. (1998): Late Permian to Late Triassic palaeomagnetic data from Iran: constraints on the migration of the Iranian block through the Tethyan Ocean and initial destruction of Pangaea. – Geophysical Journal International, **135**: 77-92.

BHATIA, M.R. (1983): Plate tectonics and geochemical composition of sandstones. – The Journal of Geology, **91**: 611-627.

BHATIA, M.R. & CROOK, K.A.W. (1986): Trace element characteristics of greywackes and tectonic setting discrimination of sedimentary basins. – Contributions to Mineralogy and Petrology, **92**: 181-193.

BLATT, H. & CHIRISTIE, J.M. (1963): Undulatory extinction in quartz of igneous and metamorphic rocks and its significance in provenance studies of sedimentary rocks. – Journal of Sedimentary Petrology, **33**: 559-579.

BLATT, H. (1967): Provenance determinations and recycling of sediments. – Journal of Sedimentary Petrology, **37**: 1311-1320.

BRUNET, M.-F., KOROTAEV, M.V., ERSHOV, A.V. & NIKISHIN, A.M. (2003): The South Caspian Basin: a review of its evolution from subsidence modelling. – Sedimentary Geology, **156**: 119-148.

CARDENAS, A., GIRTY, G.H., HANSON, A.D. & LAHREN, M.M. (1996): Assessing differences in composition between low metamorphic grade mudstones and high-grade schists using log ratio techniques. – Journal of Geology, **104**: 279-293.

CHANDLER, M.A., RIND, D. & RUEDY, R. (1992): Pangaean climate during the Early Jurassic: GCM simulations and the sedimentary record of paleoclimate. – Geological Society of America Bulletins, **104**: 543-559.

CHIU, H.-Y., CHUNG, S.-L., ZARRINKOUB, M.H., MOHAMMADI, S.S., KHATIB, M.M. & IIZUKA, Y. (2013): Zircon U-Pb age constraints from Iran on the magmatic evolution related to Neotethyan subduction and Zagros orogeny. – Lithos, **162-163**: 70-87.

CIFELLI, F., MATTEI, M., RASHID, H. & GHALAMGHASH, J. (2013): Right-lateral transpressional tectonics along the boundary between Lut and Tabas blocks (Central Iran). – Geophysical Journal International, **193**: 1153-1165.

CONDIE, K.C. (1993): Chemical composition and evolution of the upper continental crust: Contrasting results from surface samples and shales. – Chemical Geology, **104**: 1-37.

COX, R., LOWE, D.R. & CULLERS, R.L. (1995): The influence of sediment recycling and basement composition on evolution of mudrock chemistry in the southwestern United States. – Geochimica et Cosmochimica Acta, **59**: 2919-2940.

CRITELLI, S., MARSAGLIA, K.M. & BUSBY, C.J. (2002): Tectonic history of a Jurassic backarc-basin sequence (the Gran Cañon Formation, Cedros Island, Mexico), based on compositional modes of tuffaceous deposits. – Geological Society of America Bulletins, **114**: 515-527.

CULLERS, R. (1988): Mineralogical and chemical changes of soil and stream sediment formed by intense weathering of the Danburg granite, Georgia, U.S.A. – Lithos, **21**: 301-314.

CULLERS, R.L. (1994): The chemical signature of source rocks in size fractions of Holocene stream sediment derived from metamorphic rocks in the Wet Mountains region, Colorado, U.S.A. – Chemical Geology, **113**: 327-343.

CULLERS, R.L. (2000): The geochemistry of shales, siltstones and sandstones of Pennsylvanian-Permian age, Colorado, USA: implications for provenance and metamorphic studies. – Lithos, **51**: 181-203.

DAS, B.K., AL-MIKHLAFI, A.S. & KAUR, P. (2006): Geochemistry of Mansar Lake sediments, Jammu, India: Implication for source-area weathering, provenance, and tectonic setting. – Journal of Asian Earth Sciences, **26**: 649-668.

DAVOUDZADEH, M., SOFFEL, H. & SCHMIDT, K. (1981): On the rotation of the Central-East Iran microplate. – Neues Jahrbuch fur Geologie und Paläontologie, Monatshefte, **1981**: 180-192.

DICKINSON, W.R. (1970): Interpreting detrital modes of graywacke and arkose. – Journal of Sedimentary Petrology, **40**: 695-707.

DICKINSON, W.R. & SUCZEK, D.R. (1979): Plate tectonics and sandstone compositions. – American Association of Petroleum Geologists Bulletins, **63**: 2164-2182.

DICKINSON, W.R., BEARD, L.S., BRAKENRIDGE, G.R., ERJAVEC, J.L., R.C., F., INMAN, K.F., KNEPP, R.A., LINDBERG, F.A. & RYBERG, P.T. (1983): Provenance of North American Phanerozoic sandstones in relation to tectonic setting.

– Geological Society of America Bulletin, **94**: 222-235.

Dickinson, W.R. (1985): Interpreting provenance relation from detrital modes of sandstones. – In: Zuffa, G.G. (Ed.): Provenance of Arenites: 333-363; Dordrecht (Reidel Publishing Company).

Einsele, G. (2000): Sedimentary Basins: Evolution, Facies, and Sediment Budget. – 792 pp.; Berlin (Springer).

Esmaeily, D., Bouchez, J.L. & Siqueira, R. (2007): Magnetic fabrics and microstructures of the Jurassic Shah-Kuh granite pluton (Lut Block, Eastern Iran) and geodynamic inference. – Tectonophysics, **439**: 149-170.

Etemad-Saeed, N., Hosseini-Barzi, M. & Armstrong-Altrin, J.S. (2011): Petrography and geochemistry of clastic sedimentary rocks as evidences for provenance of the Lower Cambrian Lalun Formation, Posht-e-badam block, Central Iran. – Journal of African Earth Sciences, **61**: 142-159.

Folk, R.L. (1951): Stages of textural maturity in sedimentary rocks. – Journal of Sedimentary Petrology, **21**: 127-130.

Folk, R.L. (1974): Petrology of Sedimentary Rocks. – 159 pp.; Austin, Texas (Hemphill Publishing).

Fürsich, F., Wilmsen, M., Seyed-Emami, K. & Majidifard, M. (2003): Evidence of synsedimentary tectonics in the Northern Tabas Block, East-Central Iran: The Callovian (Middle Jurassic) Sikhor Formation. – Facies, **48**: 151-170.

Fürsich, F.T., Hautmann, M., Senowbari-Daryan, B. & Seyed-Emami, K. (2005a): The Upper Triassic Nayband and Darkuh formations of east-central Iran: stratigraphy, facies patterns and biota of extensional basins on an accreted terrane. – Beringeria, **35**: 53-133.

Fürsich, F., Wilmsen, M., Seyed-Emami, K., Cecca, F. & Majidifard, M. (2005b): The upper Shemshak Formation (Toarcian–Aalenian) of the Eastern Alborz (Iran): Biota and palaeoenvironments during a transgressive-regressive cycle. – Facies, **51**: 365-384.

Fürsich, F.T., Wilmsen, M., Seyed-Emami, K. & Majidifard, M.R. (2009a): Lithostratigraphy of the Upper Triassic-Middle Jurassic Shemshak Group of Northern Iran. – In: Brunet, M.-F., Wilmsen, M. & Granath, J.W. (Eds.): South Caspian to Central Iran Basins: 129-160; United Kingdom (Geological Society of London Special Publications).

Fürsich, F.T., Wilmsen, M., Seyed-Emami, K. & Majidifard, M.R. (2009b): The Mid-Cimmerian tectonic event (Bajocian) in the Alborz Mountains, Northern Iran: evidence of the break-up unconformity of the South Caspian Basin. – In: Brunet, M.-F., Wilmsen, M. & Granath, J.W. (Eds.): South Caspian to Central Iran Basins: 189-203; United Kingdom (Geological Society of London Special Publications).

Garzanti, E. & Vezzoli, G. (2003): A Classification of Metamorphic Grains in Sands Based on their Composition and Grade. – Journal of Sedimentary Reseach, **73**: 830-837.

Garzanti, E., Doglioni, C., Vezzoli, G. & Andò, S. (2007): Orogenic Belts and Orogenic Sediment Provenance. – Journal of Geology, **115**: 315-334.

Gazzi, P. (1966): Le arenarie del flysch sopra cretaceo dell'Appenninomodenese; correlazioni con il flysch di Monghidoro. – Mineralogica et Petrographica Acta, **16**: 69-97.

Ghasemi, A. & Talbot, C.J. (2006): A new tectonic scenario for the Sanandaj-Sirjan Zone (Iran). – Journal of Asian Earth Sciences, **26**: 683-693.

Golonka, J. (2004): Plate tectonic evolution of the southern margin of Eurasia in the Mesozoic and Cenozoic. – Tectonophysics, **381**: 235-273.

Grantham, J.H. & Velbel, M.A. (1988): The influence of climate and topography on rock-fragment abundance in modern fluival sands of the southern Blue Ridge Mountains, North Carolina. – Journal of Sedimentary Reseach, **58**: 219-227.

Hautmann, M. (2001): Die Muschelfauna der Nayband-Formation (Obertrias, Nor-Rhät) des östlichen Zentraliran. – Beringeria, **29**: 1-181.

Hautmann, M., Aghababalou, B. & Krystyn, L. (2011): An Unusual Late Triassic Nuculid Bivalve with Divaricate Shell Ornamentation, and the Evolutionary History of Oblique Ribs in Triassic Bivalves. – Journal of Paleontology, **85**: 22-28.

Hosseini-Barzi, M. & Shadana, M. (2010): Provenance and parental source weathering of the Khan Formation sandstone; based on petrography, modal analysis and geochemistry of major elements in Chahruf outcrop, Posht-e-Badam Block. – Quarterly Journal of Geology of Iran, **12**: 27-32 [in Persian].

Hulka, C. & Heubeck, C. (2010): Composition and Provenance History of Late Cenozoic Sediments in Southeastern Bolivia: Implications for Chaco Foreland Basin Evolution and Andean Uplift. – Journal of Sedimentary Reseach, **80**: 288-299.

Ibbeken, H. & Schleyer, R. (1991): Source and Sediment. – 286 pp.; Berlin (Springer).

Ingersoll, R.V. & Suczek, C.A. (1979): Petrology and provenance of Neogene sand from Nicobar and Bengal fans, DSDP sites 211 and 218. – Journal of Sedimentary Petrology, **49**: 1217-1228.

Ingersoll, R.V., Fullard, T.F., Ford, R.L., Grimm, J.P., Pickle, J.D. & Sares, S.W. (1984): The effect of grain size on detrital modes; a test of the Gazzi-Dickinson point-counting method. – Journal of Sedimentary Petrology, **54**: 103-116.

Johnson, C.M. & Winter, B.L. (1999): Provenance analysis of lower Paleozoic cratonic quartz arenites of the North American midcontinent region: U-Pb and Sm-Nd isotope geochemistry. – Geological Society of America Bulletins, **111**: 1723-1738.

Kroonenberg, S.B. (1994): Effects of provenance, sorting and weathering on the geochemistry of fl uvial sands from different tectonic and climatic environments. – 29th International Geological Congress: 69-81.

Leven, E.J., Davydov, V.I. & Gorgij, M.N. (2006): Pennsylvanian stratigraphy and fusulinids of central and eastern Iran. – Palaeontologia Electronica, **9.1.1A**: 1-36.

Madhavaraju, J. & Lee, Y.I. (2010): Influence of Deccan volcanism in the sedimentary rocks of Late Maastrichtian–Danian age of Cauvery basin Southeastern India: constraints from geochemistry. – Current Science, **98**: 528-537.

Mahmoudi, S., Masoudi, F., Corfu, F. & Mehrabi, B. (2010):

Magmatic and metamorphic history of the Deh-Salm metamorphic Complex, Eastern Lut block, (Eastern Iran), from U-Pb geochronology. – International Journal of Earth Sciences, **99**: 1153-1165.

Mattei, M., Cifelli, F., Muttoni, G., Zanchi, A., Berra, F., Mossavvari, F. & Eshraghi, S.A. (2012): Neogene block rotation in central Iran: Evidence from paleomagnetic data. – Geological Society of America Bulletins, **124**: 943-956.

McLennan, S.M. (1989): Rare earth elements in sedimentary rocks; influence of provenance and sedimentary processes. – Reviews in Mineralogy and Geochemistry, **21**: 169-200.

McLennan, S.M. & Taylor, S.R. (1991): Sedimentary rocks and crustal evolution: tectonic setting and secular trends. – Journal of Geology, **99**: 1-21.

McLennan, S.M., Hemming, S., McDaniel, D.K. & Hanson, G.N. (1993): Geochemical approaches to sedimentation, provenance and tectonics. – In: Johnsson, M.J. & Basu, A. (Eds.): Processes Controlling the Composition of Clastic Sediments: 21-40; Colorado (Geological Society of American Special Paper).

Middleton, G.V. (1960): Chemical composition of sandstones. – Geological Society of America Bulletins, **71**: 1011-1026.

Moosavirad, S.M., Janardhana, M.R., Sethumadhav, M.S., Moghadam, M.R. & Shankara, M. (2011): Geochemistry of lower Jurassic shales of the Shemshak Formation, Kerman Province, Central Iran: Provenance, source weathering and tectonic setting. – Chemie der Erde – Geochemistry, **71**: 279-288.

Moosavirad, S.M., Janardhana, M.R., Sethumadhav, M.S. & Prakash Narasimha, K.N. (2012): Geochemistry of Lower Jurassic sandstones of Shemshak Formation, Kerman basin, Central Iran: Provenance, source weathering and tectonic setting. – Journal of the Geological Society of India, **79**: 483-496.

Muttoni, G., Gaetani, M., Kent, D.V., Sciunnach, D., Angiolini, L., Berra, F., Garzanti, E., Mattei, M. & Zanchi, A. (2009): Opening of the Neo-tethys ocean and the pangea B to pangea A transformation during the permian. – GeoArabia, **14**: 17-48.

Najafzadeh, A., Jafarzadeh, M. & Moussavi-Harami, R. (2010): Provenance and tectonic setting of Upper Devonian sandstones from Ilanqareh Formation (NW Iran). – Revista Mexicana de Ciencias Geológicas, **27**: 545-561.

Nesbitt, H.W. & Young, G.M. (1982): Early Proterozoic climates and plate motions inferred from major element chemistry of lutites. – Nature, **299**: 715-717.

Nesbitt, H.W. & Young, G.M. (1984): Prediction of some weathering trends of plutonic and volcanic rocks based on thermodynamic and kinetic considerations. – Geochimica et Cosmochimica Acta, **48**: 1523-1534.

Pettijohn, F.J., Potter, P.E. & Siever, R. (1972): Sand and Sandstone. – 618 pp.; Berlin (Springer).

Pettijohn, F.J. (1975): Sedimentary Rocks. – 628 pp.; New York (Harper & Row).

Piper, D.Z. (1974): Rare earth elements in the sedimentary cycle: A summary. – Chemical Geology, **14**: 285-304.

Roser, B.P. & Korsch, R.J. (1988): Provenance signatures of sandstone-mudstone suites determined using discriminant function analysis of major-element data. – Chemical Geology, **67**: 119-139.

Salehi, M.A. (2012): Provenance of the siliciclastic Ab-Haji Formation: Implications for the tectonic setting of east-central Iran during the Early Jurassic. – Poster, Sedimentary Provenance Analysis (SPA) Short Course. Göttingen, Germany.

Salehi, M.A., Moussavi Harami, S.R., Mahboubi, A., Fürsich, F.T., Wilmsen, M. & Heubeck, C. (subm.): Facies associations and paleoenvironment of an extensional basin: The Lower Jurassic Ab-Haji Formation of east-central Iran. – Journal of Asian Earth Sciences.

Salehi, M.A. (2013): Palaeogeography of Early Jurassic in east-central Iran considering the Ab-Haji Formation. – The 7th Symposium of Iranian Paleontological Socieity, Esfahan-Iran, 22-24 May (in Persian): 101-105.

Senowbari-Daryan, B., Rashidi, K. & Torabi, H. (2010): Foraminifera and their associations of a possibly Rhaetian section of the Nayband Formation in central Iran, northeast of Esfahan. – Facies, **56**: 567-596.

Seyed-Emami, K. (1971): The Jurassic Badamu Formation in the Kerman region, with some remarks on the Jurassic stratigraphy of Iran. – Geological Survey of Iran, Report, **19**: 1-80.

Seyed-Emami, K., Schairer, G., Fürsich, F.T., Wilmsen, M. & Majidifard, M.R. (2000): First record of ammonites from the Badamu formation at the Shotori Mountains (Central Iran). – Eclogae Geologicae Helvetiae, **93**: 257-263.

Seyed-Emami, K. (2003): Triassic in Iran. – Facies, **48**: 91-106.

Seyed-Emami, K., Fürsich, F.T., Wilmsen, M., Schairer, G. & Majidifard, M.R. (2004a): First record of Jurassic (Toarcian – Bajocian) ammonites from the northern Lut Block, east-central Iran. – Acta Geologica Polonica, **54**: 77-94.

Seyed-Emami, K., Fürsich, F.T. & Wilmsen, M. (2004b): Documentation and significance of tectonic events in the Northern Tabas block (East-Central Iran) during the Middle and Late Jurassic. – Rivista Italiana di Paleontologia e Stratigrafia, **110**: 163-171.

Shadan, M. & Hosseini-Barzi, M. (2013): Petrography and geochemistry of the Ab-e-Haji Formation in Central Iran: implications for provenance and tectonic setting in the southern part of Tabas block. – Revista Mexicana de Ciencias Geológicas, **30**: 80-95.

Soffel, H. & Forster, H. (1984): Polar wander path of the Central East Iran microplate including new results. – Neues Jahrbuch für Geologie und Paläontologie, Abhandlungen, **168**: 165-172.

Soffel, H., Davoudzadeh, M., Rolf, C. & Schmidt, S. (1996): New palaeomagnetic data from Central Iran and a Triassic palaeoreconstruction. – Geologische Rundschau, **85**: 293-302.

Stampfli, G.M. & Borel, G.D. (2002): A plate tectonic model for the Paleozoic and Mesozoic constrained by dynamic plate boundaries and restored synthetic oceanic isochrons. – Earth and Planetary Science Letters, **196**: 17-33.

Stöcklin, J. (1974): Possible ancient continental margins in Iran. – In: Burke, C.A. & Drake, C.L. (Eds.): The

Geology of Continental Margins: 873-887; New York (Springer).

Suttner, L.J., Basu, A. & Mack, G.H. (1981): Climate and the origin of quartz arenites. – Journal of Sedimentary Petrology, **51**: 1235-1246.

Suttner, L.J. & Dutta, P.K. (1986): Alluvial sandstone composition and paleoclimate; I, Framework mineralogy. – Journal of Sedimentary Reseach, **56**: 329-345.

Taylor, S.R. & McLennan, S.M. (1985): The Continental Crust: Its Composition and Evolution. – 312 pp.; Oxford (Blackwell).

Thierry, J. (2000): Late Sinemurian (193-191 Ma). – In*:* Dercourt, J., Gaetani, M., Vrielynck, B., Barrier, E., Biju-Duval, B., Brunet, M.-F., Cadet, J., Crasquin, S. & Sandulescu, M. (Eds.): Atlas Peri-Tethys palaeogeographical maps: 49-59; Paris (Commission for the Geological Map of the World; CGMW / CCGM).

Tortosa, A., Palomares, M. & Arribas, J. (1991): Quartz grain types in Holocene deposits from the Spanish Central System: some problems in provenance analysis. – In*:* Morton, A.C., Todd, S.P. & Huaghton, P.D.W. (Eds.): Development in Sedimentary Provenance Studies: 47-54; United Kingdom (Geological Society of London Special Publications).

Visser, J.N.J. & Young, G.M. (1990): Major element geochemistry and paleoclimatology of the Permo-Carboniferous glacigene Dwyka Formation and postglacial mudrocks in southern Africa. – Palaeogeography, Palaeoclimatology, Palaeoecology, **81**: 49-57.

von Eynatten, H., Barceló-Vidal, C. & Pawlowsky-Glahn, V. (2003): Composition and Discrimination of Sandstones: A Statistical Evaluation of Different Analytical Methods. – Journal of Sedimentary Reseach, **73**: 47-57.

Weltje, G.J., Meijer, X.D. & De Boer, P.L. (1998): Stratigraphic inversion of siliciclastic basin fills: a note on the distinction between supply signals resulting from tectonic and climatic forcing. – Basin Research, **10**: 129-153.

Wilmsen, M., Fürsich, F.T. & Seyed-Emami, K. (2003): Revised lithostratigraphy of the Middle and Upper Jurassic Magu Group of the northern Tabas Block, east-central Iran. – Newsletters on Stratigraphy, **39**: 143-156.

Wilmsen, M., Wiese, F., Seyed-Emami, K. & Fürsich, F.T. (2005): First record and significance of Turonian ammonites from the Shotori Mountains, east-central Iran. – Cretaceous Research, **26**: 181-195.

Wilmsen, M., Fürsich, F.T., Seyed-Emami, K., Majidifard, M.R. & Taheri, J. (2009a): The Cimmerian Orogeny in northern Iran: tectono-stratigraphic evidence from the foreland. – Terra Nova, **21**: 211-218.

Wilmsen, M., Fürsich, F.T., Seyed-Emami, K. & Majidifard, M.R. (2009b): An overview of the stratigraphy and facies development of the Jurassic System on the Tabas Block, east-central Iran. – In*:* Brunet, M.-F., Wilmsen, M. & Granath, J.W. (Eds.): South Caspian to Central Iran Basins: 323-343; United Kingdom (Geological Society of London Special Publications).

Wilmsen, M., Fürsich, F., Seyed-Emami, K., Majidifard, M. & Zamani-Pedram, M. (2010): Facies analysis of a large-scale Jurassic shelf-lagoon: the Kamar-e-Mehdi Formation of east-central Iran. – Facies, **56**: 59-87.

Zamani-Pedram, M. (2011): Source, facies, and sedimentary environments of the Middle to Upper Jurassic strata in the Kerman and Tabas areas, east-central Iran. – 212 pp., PhD, Julius-Maximilians-Universität Würzburg.

Manuscript received: May 20th, 2013.
Revised version accepted by the Bonn editor: October 2nd, 2013.

Addresses of the authors:

Mohammad Ali Salehi, Seyed Reza Moussavi-Harami, Asadollah Mahboubi , Department of Geology, Faculty of Sciences, Ferdowsi University of Mashhad, 91775-1436 Mashhad, Iran;
(email: ma.salehi@stu-mail.um.ac.ir

Markus Wilmsen, Senckenberg Naturhistorische Sammlungen Dresden, Museum für Mineralogie und Geologie, Sektion Paläozoologie, Königsbrücker Landstr. 159, 01109 Dresden, Germany.

Christoph Heubeck, Freie Universität Berlin, Department of Geological Sciences, Malteserstr. 74-100, 12249 Berlin, Germany.